CHAPTER 1

LITERATURE REVIEW

Chapter (1)

1-1- Catalysis, Kinetics and Selectivity of the Fischer-Tropsch Synthesis

The chemistry of fischer-tropsch synthesis involves the hydrogenation of carbon monoxide, in which a broad spectrum of products, including paraffins (alkanes), olefins (alkenes), alcohols, aldehydes, ketons, acids, esters, etc. are produced. Aromatic compounds in small amounts are also formed by secondary dehydocyclization reactions from the primary hydrocarbons

1-1-1- Fischer-Tropsch Catalysts

The most common Fischer-Tropsch catalysts are group VIII metals (Co, Ru, and Fe). Iron catalysts are commonly used, because of their low costs in comparison to other active metals. Most early FT catalysts were prepared with precipitation techniques **[Anderson, 1956].** Novel catalyst preparation methods are sintering and fusing metal oxides with desired promoters. Alkali-promoted iron catalysts have been applied industrially for the Fischer-Tropsch synthesis during many years **[Rao et al., 1992].** These catalysts have a high water gas shift activity, high selectivity to olefins and appear to be stable when synthesis gas with a high H_2/CO ratio is converted **[Kolbel and Ralek, 1980 and Jager and Espinoza, 1995].**

Cobalt catalysts give the highest yields and longest lifetime and produce predominantly linear alkanes **[Chaumette et al., 1995].** A precipitated cobalt catalyst on kieselguhr (Ruhrchemie) became the standard catalyst for commercial purposes in the Second World War in Germany **[Frohning et al., 1977].** Cobalt catalysts are not inhibited by water, resulting in a higher productivity at a high synthesis gas conversion **[Berge van and Everson, 1997].**

Ruthenium is a very active but expensive catalyst for the Fischer-Tropsch synthesis relative to Co and Fe. Cobalt and ruthenium catalysts are not very active towards the WGS reaction in contrast to most iron-based Fischer-Tropsch catalysts

[Newsome, 1980]. The water gas shift (WGS) reaction is important when synthesis gas with non-stoichiometric amounts of hydrogen is used.

1-1-2- Mechanism of the Fischer-Tropsch Synthesis

The FTS is a polymerization reaction with the following steps **[Adesina, 1996]**:

1.Reactant adsorption;

2. Chain initiation;

3. Chain growth;

4. Chain termination;

5. Product desorption;

6. Readsorption and further reaction.

A variety of surface species were proposed to describe chain initiation and chain growth. **(Figure 1.1)** gives an overview of observed and postulated species on the catalyst surface during Fischer Tropsch synthesis.

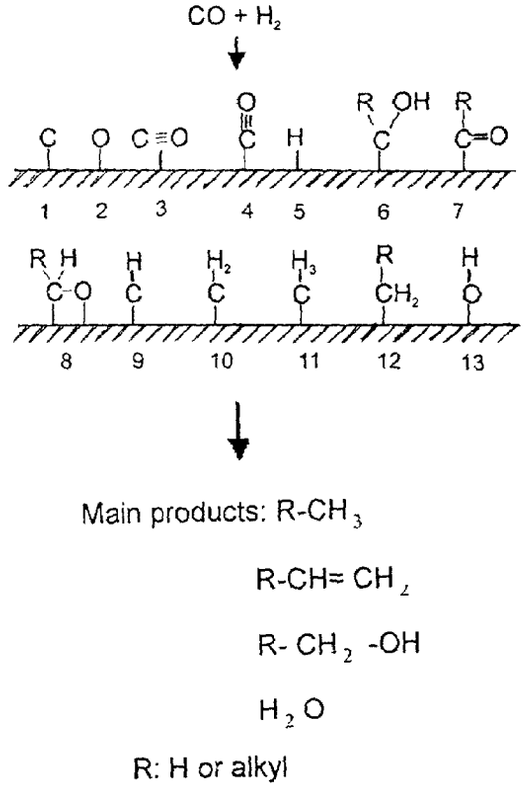

Figure 1.1 Observed and postulated chemisorbed species during Fischer-Tropsch Synthesis **[Schulz et al., 1988 a].**

The most important growth mechanism for the hydrocarbon formation on cobalt **[Chaumette et al., 1995]**, iron **[Biloen et al., 1979 and Dictor and Bell, 1986]**, and ruthenium catalysts **[Biloen et al., 1979 and Chuang et al., 1985]** is the surface carbide mechanism by CH_2 insertion **[Fischer and Tropsch 1923; Wojciechowski, 1988; and Schulz et al., 1993]. Figure (1.2)** shows a schematic representation of the initiation, growth and termination of chains according to this mechanism. The set of elementary reactions proposed for the formation of linear hydrocarbons is given in **(table 1.1).**

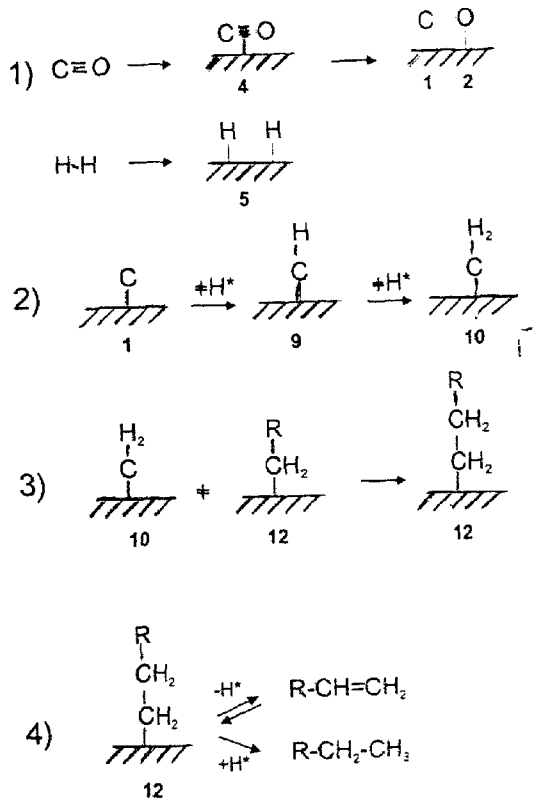

Figure 1.2 Carbide mechanism for the Fischer-Tropsch synthesis **[Bell, 1981 and Sarup and Wojciechowski, 1989].**

Table 1.1 Proposed mechanism of the hydrocarbon synthesis from CO and H_2 **[Bell, 1981 and Wojciechowski, 1988; Lox and froment, 1993 b and Hovi et al., 1995].**

Adsorption	
1	$CO + s \longleftrightarrow COs$
2	$COs + s \longleftrightarrow Cs + Os$
3	$H_2 + 2s \longleftrightarrow 2Hs$
Surface reactions	
Water formation	
4	$Os + Hs \longrightarrow HOs + s$
5	$HOs + Hs \longrightarrow H_2O + 2s$
Or	$Os + H_2 \longrightarrow H_2O + s$
Chain initiation	
6	$Cs + Hs \longleftrightarrow CHs + s$
7	$CHs + Hs \longleftrightarrow CH_2s + s$
8	$CH_2s + Hs \longleftrightarrow CH_3s + s$
Or	$COs + H_2 \longleftrightarrow CHOHs$
	$CHOHs + H_2 \longleftrightarrow CH_2s + H_2O$
9 Methanation	$CH_3s + Hs \longrightarrow CH_4 + s$
10 Chain growth	$C_nH_{2n+1}s + CH_2s \longrightarrow C_{n+1}H_{2n+3}s + s$
11-Hydrogenation to Paraffins	$C_nH_{2n+1}s + Hs \longrightarrow C_nH_{2n+2} + 2s$
12-β-dehydrogenation to olefins	$C_nH_{2n+1}s \longleftrightarrow C_nH_{2n} + Hs$

1-1-3- Water Gas Shift Reaction

The WGS reaction over unsupported magnetite proceeds via a direct oxidation mechanism, while all supported iron catalysts operate via a mechanism with formate species due to limited change of oxidation state of the iron cations. A mechanism based on a reactive formate intermediate is shown in **Figure (1.3) [Oki and Mezaki, 1973; Rethwisch and Dumesic, 1986; Graaf et al., 1988 and Lox and Forment, 1993 b].** The formate intermediate is reduced to adsorbed or gaseous carbon dioxide. Direct oxidation of adsorbed or gas-phase CO to CO_2 is presented in **figure 1-4 [Sachtler, 1982; Rethwisch and Dumesic, 1986; Xu and Froment 1989; Chinchen et al., 1990; Ovesen et al., 1996 and Vandenbussche and Froment 1996].**

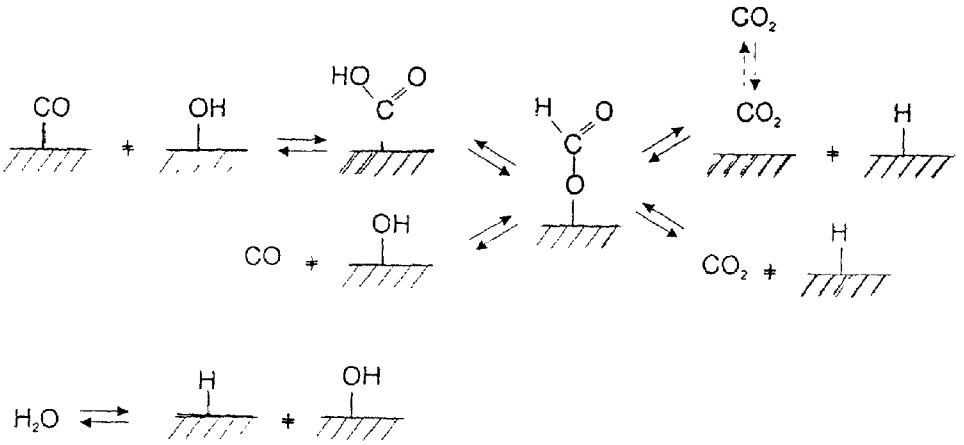

Figure 1.3 Water gas shift reaction mechanism via formate species **[Lox and Froment, 1993 b].**

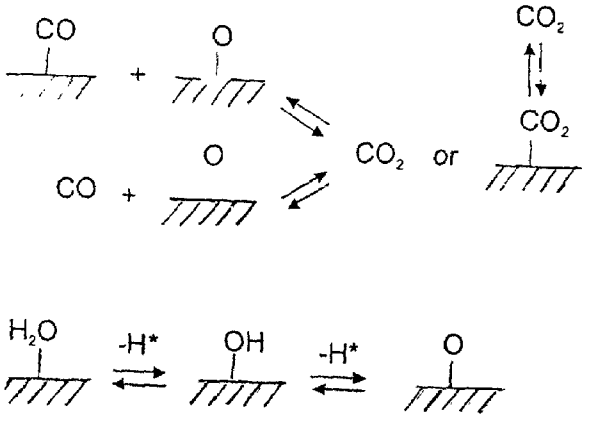

Figure 1.4 Water gas shift mechanism via direct oxidation**[Lox and Froment, 1993b]**

1-1-4-Kinetics

The Fischer-Tropsch synthesis can be simplified as a combination of the FT reaction and the water gas shift (WGS) reaction. Water is a primary product of the FT reaction, and CO_2 can only be produced by the WGS reaction ($R_{WGS} = R_{CO_2}$). The water gas shift reaction is a reversible parallel-consecutive reaction with respect to CO **figure (1-5).**

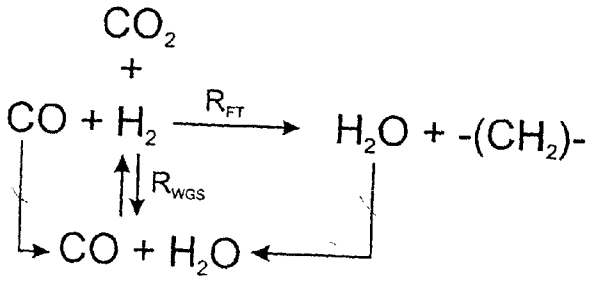

Figure 1.5 Scheme of the reaction of carbon monoxide and hydrogen.

Or

$$CO + (1+m/2n)\,H_2 \rightarrow 1/n\,C_nH_m + H_2O\ (FT) \qquad -\Delta H_{FT} = 165\ kj/mol \qquad 1\text{-}1$$

$$CO + H_2O \longleftrightarrow CO_2 + H_2\ (WGS) \qquad -\Delta H_{WGS} = 41\ kj/mol \qquad 1\text{-}2$$

Where n is the average carbon number and m is the average number of hydrogen atoms of the hydrocarbon products. The WGS activity can be high over potassium-promoted iron catalysts and is negligible over cobalt or ruthenium catalysts.

The major problem in describing Fischer-Tropsch reaction kinetics is the complexity of its reaction mechanism and the large number of species involved. Most studies aim at catalyst improvement and postulate empirical power law kinetics for the carbon monoxide rates **[Dry, 1981 and Ribeiro et al, 1997]:**

$$-R_{CO} = k\,P_{H_2}^{a}\,P_{CO}^{b} \qquad (1\text{-}3)$$

and carbon dioxide formation or water gas shift reaction **[Bub and Baerns, 1980 and Newsome, 1980]:**

$$R_{CO2} = k\, P_{H_2O}^{c}\, P_{CO}^{d} \qquad (1\text{-}4)$$

Some authors derived Langmuir-Hinshelwood- Hougen-Watson (LHHW) rate expressions for the reactant consumption **[Wojciechowski, 1988 and Lox and Forment, 1993 b].** In most cases the rate determining step was assumed to be the formation of the building block or monomer, methylene **[Dry, 1976; Atwood and Bennett, 1979; Dixit and Tavlarides, 1983; Huff and Satterfield, 1984; Sarup and Wojciechowski, 1989; Nettelhoff et al., 1985 and Zimmerman and Bukur, 1990]**.

Kinetic equations can be based on the overall synthesis gas consumption $-R_{H_2+CO} = -R_{CO} - R_{H_2}$, which is independent of the WGS equilibrium, or based on CO consumption to hydrocarbon products ($R_{FT} = -R_{CO} - R_{WGS}$). The rate of synthesis gas consumption only differs from the FT reaction rate by reaction stoichiometry, $-R_{H_2+CO} = (2 + m/2n)R_{FT}$. Reaction rate equations used to be expressed in either liquid phase concentrations or, preferably, in gas phase partial pressures. Since Henry's constants are temperature dependent, activation energies will also be influenced by the use of either liquid or gas concentration terms **[Zimmerman and Bukur, 1990 and Nettelhoff et al., 1985].**

The Fischer-Tropsch activity of Fe and Co depends on the preparation method, metal loading of the catalyst, and catalyst support **[Snel, 1989; Martin and Vannice, 1991; Iglesia et al., 1992; Kuipers et al 1995 and Ribeiro et al., 1997].**

1-1-4-1- Kinetic Rate Equations

a- Iron Based Catalysts

In general for iron catalysts, the FT reaction rate increases with H_2 partial pressure and decreases with partial pressure of water. The mechanistic kinetic rate expressions for iron catalysts are all based on the formation of the monomer species formed by either the carbide mechanism or the combined enol/carbide mechanism as the rate-determining step in the consumption of synthesis gas.

The water gas shift can increase or decrease the Fischer-Tropsch synthesis reaction rate by altering the concentrations of the reactants and products. It is

generally accepted that the WGS and FT reactions proceed on different active sites on precipitated iron catalyst. CO_2 inhibition is not as strong as water inhibition due to the large difference in adsorption coefficients [**Dry et al., 1969 and Zimmerman and Bukur, 1990**]. However, iron catalysts with a high activity of the water gas shift reaction convert a significant amount of water into CO_2.

b- Cobalt Based Catalysts

Only a few kinetic studies on cobalt-based catalysts are available, **table 1.3**. Remarkably, nearly all-kinetic expressions developed for cobalt-based catalysts have a different form than for iron based catalysts, **table 1.2**. Generally, these kinetic equations are based on a rate-determining step, which involves a dual-site surface reaction, resulting in a quadratic denominator in the rate expression. Furthermore, inhibition terms of H_2O on cobalt catalysts are not found. Because the WGS reaction hardly plays a role on cobalt, no CO_2 is formed.

Kinetic studies of the FTS on iron and cobalt catalysts are summarized in **table 1.2.** The corresponding operating conditions are given **(table 1.3).** It can be seen that the pressure dependency of CO and H_2 in the numerator ranges from 1/2 to 1, and 1/2 to 2, respectively. The denominator is quadratic in case of a dual site elementary reaction, in contrast to a single site rate-determining step.

c- Water Gas Shift Kinetics

Individual WGS kinetics has been studied extensively [**Newsome, 1980; Grenoble et al., 1981 and Ovesen et al., 1996**], sometimes in combination with the methanation reaction [**Xu and Froment, 1989**]. Kinetic studies of the WGS reaction under FT conditions on iron-based catalysts are summarized in **(table 1.4).** Since the WGS reaction is an equilibrium reaction at or close to equilibrium under Fischer-Tropsch reaction conditions the reverse reaction has to be taken into account. For the temperature dependency of the equilibrium constant of the WGS reaction, K_P, the following relation can be used [**Graaf et al., 1986**]:

$$\text{Log K}_P = \log\left(\frac{P_{CO_2}P_{H_2}}{P_{H_2O}P_{CO}}\right)_{eq} = \left(\frac{2073}{T}\right) - 2.029 \qquad (1\text{-}5)$$

Table 1.2 Reaction rate equations overall synthesis gas consumption rate, proposed in the studies mentioned in **Table 1.3.**

	Kinetic expression	References
a)	$k P_{H_2}$	**[Anderson, 1956; Zimmerman and Bukur, 1990 and Dry et al., 1972]**
b)	$k P_{H_2}^{a} P_{CO}^{b}$	**[Bub and Baerns, 1980]**
c)	$\frac{kP_{H_2} P_{CO}}{P_{CO} + aP_{H_2O}}$	**[Anderson, 1956; Zimmerman and Bukur, 1990; Dry, 1976; Atwood and Bennett, 1979 and Shen et al., 1994]**
d)	$\frac{kP_{H_2}^2 P_{CO}}{P_{CO}P_{H_2} + aP_{H_2O}}$	**[Dry, 1976; Huff and Satterfield, 1984; Deckwer et al., 1986; Whiters et al., 1990 and Shen et al., 1994]**
e)	$\frac{kP_{H_2}^2 P_{CO}}{1 + aP_{CO}P_{H_2}^2}$	**[Anderson, 1956]**
f)	$\frac{kP_{H_2} P_{CO}}{P_{CO} + aP_{CO_2}}$	**[Zimmerman and Bukur, 1990; Netterlhoff et al., 1985; Deckwer et al, 1986; Ledawkowicz, 1985]**
g)	$\frac{kP_{H_2} P_{CO}}{P_{CO} + aP_{H_2O} + bP_{CO_2}}$	**[Zimmerman and Bukur, 1990; Netterlhoff et al., 1985; Deckwer et al., 1986; Ledakow1cz et al., 1985]**
h)	$\frac{kP_{CO}^{1/2} P_{H_2}^{1/2}}{(1 + a P_{CO}^{1/2} + bP_{H_2}^{1/2})^2}$	**[Sarup and wojcieshowski, 1989]**
i)	$\frac{kP_{CO} P_{H_2}^{1/2}}{(1 + a P_{CO} + bP_{H_2}^{1/2})^2}$	**[Wojcieshowski, 1988]**
j)	$\frac{kP_{CO} P_{H_2}}{(1 + bP_{CO})^2}$	**[Dixit and Tavlarides, 1983; Chanenchuk, 1991 and Yates and Satterfield, 1991]**
k)	$\frac{kP_{CO} P_{H_2}^{1/2}}{(1 + a P_{CO} + bP_{H_2O})^2}$	**[Gerard vander-laan and Beennacker 2000]**

Table 1-3 Kinetics studies for the FT on cobalt and iron catalysts.

Catalyst	Reactor	Operating conditions			Kinetic Exp.	Refernces.
		T, ^{0}C	P, Mpa	H_2/CO feed		
Fused Fe/ K	Fixed bed	225- 265	1.0- 1.8	1.2- 7.2	(a)	**[Dry et al., 1972]**
Prec. Fe/ K/CU	Slurry	235-265	1.5- 3.0	0.6-1.0	(a)	**[Zimmerman and Bukur, 1990]** [1]
Prec. Fe/ K/CU	Slurry	250	1.5- 3.0	0.6- 1.0	(c)	**[Zimmerman** and **Bukur, 1990]**
Iron	Fixed bed	?	?	?	(c)	**[Anderson, 1956]**
Fused Fe/ K	Gradientless	250- 315	2.0	2.0	(c)	**Atwood and Benett, 1979]**
fixed bed /Fused iron	Slurry	232-263	0.4-1.5	0.5-1.8	(d)	**[Huff and Satterfield, 1984]**
Prec. Iron	Slurry	220- 260	1.0	0.5- 0.6	(f)	**[Ledakowicz, 1985]**
Prec. Iron	Slurry	220- 280	0.5- 1.2	0.5- 3.5	(c)	**[Nettelhoff et al., 1985]**
Fused iron	Slurry	210- 270	.5- 5.5	0.5- 3.5	(f)	**[Nettelhoff et al., 1985]**
Co/ Kieselguhr	Berty	190	0.2- 1.5	0.5- 8.3	(h, i)	**[Wojcieshowski, 1988]** [2], **Sarup and Wojcieshowski**
Co/ MgO/ SiO_2	Slurry	220- 240	1.5- 3.5	1.5-3.5	(j)	**[Yates and Saterfield, 1991]** [3]
Co/ Zr/ SiO 2	Slurry	220- 280	2.1	0.5- 2.0	(d)	**[Whiters et al., 1990]**
Prec. Fe/ Cu/ K	Gradientless	230- 264	1.0- 2.6	1.1-2.4	(d)	**[Shen et al., 1994]**
Prec. Fe/ Cu/ K	Gradientless	230- 264	1.0-2.6	1.1-2.4	(c)	**[Shen et al., 1994]**
Prec. iron	Slurry	220- 260	-	0.5- 0.8	(f)	**[Deckwer et al., 1986]** [2]
Prec. Iron	Slurry	220- 260	-	0.8- 2.0	(c)	**[Deckwer et al., 1986]** [2]
Prec. Iron	Fixed bed	250-350	0.6- 2.1	3.0-6.0	-	**[Lox and froment, 1993 b]**
Fe/Cu/K/Sio_2	Slurry	250	0.8-4	0.25-4	K	**[Gerard and Vander - laan, 2000]**

[1] No temperature dependence of optimal rate equations (c) (Fe/ Cu/ K) and (g) (100 Fe/ 0.3 Cu/ 0.2 K) is given

[2] Rate equations expressed in liquid concentrations

[3] Only measurements at 190 °C are reported. Conversions and space velocities are not mentioned by **[Sarup and Wojciechowski, 1989]**

Table 1.4 Summary of kinetic studies of the WGS reaction

Kinetic Expression	E_A (kw) (Kj/mole)	References
$R_{WGS} = k_W (P_{H_2O} P_{CO} - P_{CO_2} P_{H_2} / K_P)$		**[Zimmerman & Bukur , 1990]**[1]
$R_{WGS} = k_W P_{CO}$	124[1]	**[Dry, 1976; Feimer et al., 1981 and Zimmerman and Bukur, 1990]**
$R_{WGS} = \frac{k_W (P_{H_2O} P_{CO} - P_{CO_2} P_{H_2}^{1/2} / K_P)}{(1 + a P_{H_2O} / P_{H_2}^{1/2})^2}$	27.7	**[Lox and froment, 1993 b]**
$R_{WGS} = \frac{k_W (P_{H_2O} P_{CO} - P_{CO_2} P_{H_2} / K_P)}{P_{CO} P_{H_2} + a P_{H_2O}}$	88[2]	**[Zimmerman & Bukur, 1990 and Shen et al., 1994]**
$R_{WGS} = \frac{k_W (P_{H_2O} P_{CO} - P_{CO_2} P_{H_2} / K_P)}{(P_{CO} + a P_{H_2O} + b P_{CO_2})}$	125[2]	**[Zimmerman & Bukur, 1990 and Shen et al., 1994]**
$R_{WGS} = \frac{k_W (P_{H_2O} P_{CO} - P_{CO_2} P_{H_2} / K_P)}{(1 + k_1 P_{CO} + k_3 P_{H_2O})^2}$		**[Gerard vander-laan and Beennacker 2000]**

[1] Activation energy **[Feimer et al., 1981]**

[2] Activation energy **[Shen et al., 1994]**

1-1.5-Selectivity of the Fischer-Tropsch Synthesis

The products from the FTS on Co, Fe, and Ru show the following characteristics **[Anderson, 1984; Wojciechowski, 1988; Madon et al., 1993]:**

1. The carbon-number distributions for hydrocarbons give the highest concentration for C_1 and decreases monotonically for higher carbon numbers, though around C_3-C_4 often a local maximum is observed.

2. Monomethyl-substituted hydrocarbons are present in moderate amounts while dimethyl products are present in significantly smaller amounts than monomethyl.

None of these branched products contain quaternary carbon atoms **[Anderson, 1984].**

3. Olefins from iron catalysts exceed 50% of the hydrocarbon products at low carbon numbers, and more than 60% of these are α-olefins. The ethene selectivity is low in comparison to propene. The olefin content decreases asymptotically to zero with increasing carbon number on Co, Ru, and Fe catalysts. For cobalt catalysts both the fraction of total olefins and α-olefins are smaller, and both decrease with carbon number.

4. A change in chain growth parameter in the distribution is only observed for linear paraffins and not for olefins.

5. Yields of alcohols are maximal at C_2 and decrease with carbon number. Low yields of methanol are probably the result of thermodynamic limitations.

1-1-5-1. Influence of Process Conditions on the Selectivity

The process conditions such as temperature, partial pressures of H_2 and CO, time on stream as well as the composition and reduction of the catalyst influence the product selectivity. **Table 1.5** shows the general influence of different parameters on the selectivity. The influence of the synthesis gas conversion on the product selectivity is strongly related to the influence of the process conditions.

a- Temperature

Increase of temperature results in a shift towards products with a lower carbon number on iron **[Dictor and Bell, 1986 and Donnelly and Satterfield, 1989],** ruthenium **[Dry, 1981,** and cobalt **[Dry, 1981]** catalysts.

b- Partial pressure of H_2 and CO

Most studies show that the product selectivity shifts to heavier products and to more oxygenates with increasing total pressure **[Dry, 1981].** Increasing H_2/CO ratios in the reactor result in lighter hydrocarbons and a lower olefin content **[Dictor and Bell, 1986 and Donnelly and Satterfield, 1989].**

c- Space velocity

An increase of the olefin to paraffin ratio with increasing space velocity (thus a decrease of the conversion) was observed. The selectivity to methane and olefins

decreases with a decrease of the space velocity, while the selectivity towards paraffins remains unchanged.

d- Time on stream

The selectivity to the production of methane, low molecular products and oxygenate increases with time on stream. The selectivity changes with time can be caused by the formation of carbonaceous deposits on sites with potassium promoters **[Dry, 1981].** Sintering of precipitated iron catalysts lead to reduction of the surface area. Also Deactivation of catalysts during the FTS may affect the activity and selectivity to hydrocarbon products. Agglomeration of initially small crystallites is enhanced by high water pressures.

e-Reduction of the catalyst

The hydrocarbon selectivity appeared to relate strongly on the pretreatment procedure. Low methane and C_2-C_4 selectivities and high diesel fuel and wax (C_{12+}) selectivities were observed at pretreatments with CO and CO/H_2. Reduction at 280°C causes a shift to products with higher carbon number relative to 250°C. Olefin selectivities are reported to decrease after hydrogen reduction in comparison to reduction with CO or synthesis gas.

1-1-5-2- Product Selectivity Models

The FT synthesis has been recognized as a polymerization reaction **[Adesina,1996].** The reactants, CO and H_2, adsorb and dissociate at the surface of the catalyst and react to form chain initiator (CH_3), and methylene monomer (CH_2) and H_2O. The most important growth mechanism for the hydrocarbon formation is the surface carbide mechanism by CH_2 insertion into adsorbed alkyl chains. Termination can take place by dehydrogenation to an α-olefin or hydrogenation to form a paraffin **[Anderson, 1956; Bell, 1981 and Dry, 1981].**

1- Anderson-Schulz-Flory Distribution Model

According to **[Anderson, 1956]** the distribution for n-paraffins can be described by the Anderson-Schulz-Flory (ASF) equation:

$$m_n = (1-\alpha_S)\,\alpha_S^{\,n-1} \quad \text{and} \quad \frac{w_n}{n} = \frac{(1-\alpha_S)^2}{\alpha_S}\alpha_S^{\,n} \tag{1-6}$$

Where the growth probability factor α_S is independent of n, m_n is the mole fraction of a hydrocarbon with chain length n, α is defined by:

$$\alpha_S = \frac{R_p}{R_p + R_t} \tag{1-7}$$

Where R_p and R_t are the rate of propagation and termination, respectively. α_S determines the total carbon number distribution of the FT products. The range of α_S is dependent on the reaction conditions and catalyst type. **Dry [1982a]** reported typical ranges of α_S on Ru, Co, and Fe of: 0.85- 0.95, 0.70-0.80, and 0.50- 0.70, respectively. The chain growth probability, α_S, decreases with an increase of the reactor temperature **[Everson, 1978; Dry, 1982b; Dictor and Bell, 1986; Donnelly and Satterfield, 1989 and Lox and Froment, 1993 b].** A decrease of α is observed at higher H_2/CO ratios **[Bell, 1981; Dictor and Bell, 1986; Donnelly and Satterfield. 1989 and Lox and Froment, 1993 a].**

Table 1.5 Selectivity control in Fischer-Tropsch synthesis by process conditions and catalyst modifications from **[Roper, 1983].**

Parameter	Chain Length	Chain branching	Olefin select.	Alcohol select.	Carbon Deposition	Methane select.
Temperature	↓	↑	*	↓	↑	↑
Pressure	↑	↓	*	↑	*	↓
H_2/CO	↓	↑	↓	↓	↓	↑
Conversion	*	*	↓	↓	↑	↑
Space velocity	*	*	↑	↑	*	↓
Alkali content						
Iron catalyst	↑	↓	↑	↑	↑	↓

↑ increases ↓ decreases * not affected

Figure 1-6 shows the growing mechanism for a constant α. The ASF equation does not distinguish between different product types. **Glebov and Kliger [1994]** showed that the original Anderson-Schulz-Flory equation (Eq. **1-6**) could be modified for the description of multicomponent FT products. The mole fraction of a product, component type (paraffins, olefins, alcohols, and so forth) *i* with carbon number *n* can be calculated from:

$$\sum^{i} m_n^i = (1-\alpha_S)\,\alpha_S^{\,n-1} \tag{1-8}$$

The usual deviations of the distribution of α-olefins and paraffins are a relatively high yield of methane **[Wojciechowski, 1988; Schulz et al., 1993; Komaya, 1994 and Kuipers et al, 1996]** and a relatively low yield of ethene **[Novak et al., 1981; Wojciechowski, 1988 and Komaya, 1994]** in comparison to the ASF distribution. Higher surface mobility or reactivity of C_1 and C_2 precursors and rapid readsorption of ethane give the most reasonable explanation for the deviations of the short-chain hydrocarbons from the ASF distribution. Furthermore, an exponential decrease of the α-olefin to paraffin ratio and change in chain growth parameter α_n; with increasing chain length is observed. These deviations are caused by secondary reactions, readsorption and hydrogenation, of α-olefins **[Iglesia et al., 1993 a, b; Komaya, 1994 and Kuipers et al, 1995]**. However, secondary hydrogenation is strongly inhibited by CO and H_2O in comparison to readsorption **[Iglesia et al.,** 1993 a, b].

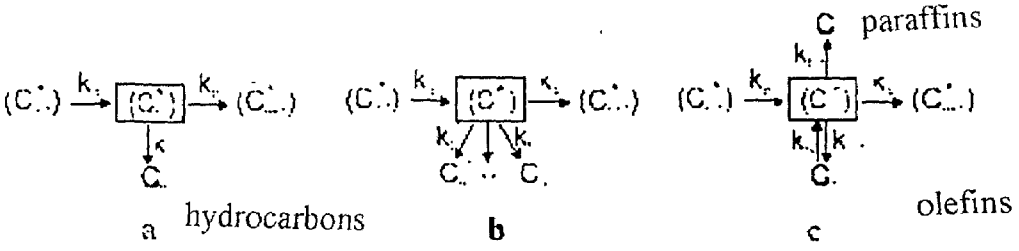

Figure 1-6 Reaction growth schemes Fischer-Tropsch synthesis

a. Classical Anderson-Schulz-Flory model with one termination constant for all products.

b. Multiple termination probabilities originating from a single intermediate.

c. Termination to paraffins and olefins, whereas the latter can be readsorbed on the catalytic surface.

Readsorption of α-olefins leads to chain initiation and will result in a decrease of the olefin to paraffin ratio and increase of the chain growth parameter with chain length. The olefin readsorption rate depends on chain length due to increasing physisorption on the catalyst surface and increasing solubility in FT wax with chain length **[Komaya, 1994 and Kuipers et al., 1995].**

A new product distribution model, called α-Olefin Readsorption Product Distribution Model (ORPDM) was proposed and tested by **[Gerard vander-laan and Beennacker 2000]** to explain the deviations from the ASF distribution. The new model combines a mechanistic model of olefin readsorption with kinetics of chain growth and termination on the same catalytic sites.

2-α-Olefin Readsorption Product Distribution Model (ORPDM)

The α-Olefin Readsorption Product Distribution Model **(ORPDM)** accounts for secondary readsorption of α-olefins on FT growth sites (**Fig 2-7**). Here, CO_G and CO_S denote the gas phase and the adsorbed CO, respectively. $C_{M,S}$ refers to adsorbed monomeric building units ($CH_{2,S}$), and $C_{n,S}$ is an adsorbed alkyl species with carbon number n. Chain growth initiates by hydrogenation of $C_{M,S}$ to $CH_{3,S}$ while chain propagation proceeds via insertion of $C_{M,S}$ into adsorbed alkyl chains. Chain termination by dehydrogenation of adsorbed alkyl chains gives olefins, whereas paraffins are formed by hydrogenation of alkyl species **[Krishna and Bell, 1993 and Komaya, 1994].** Based on the reaction network shown in **figure (1.7)**, α-olefins may readsorb on growth sites and continue to grow via propagation with monomers or terminate as hydrocarbon product **[Iglesia et al., 1993 a, b and Komaya, 1994].**

The fractional surface coverage (θ) could be calculated by the following equations:

$$\frac{\theta_2}{\theta_1} = \frac{p}{t_0^2/(1+k_R^2)+t_p^2+p} = \alpha_2 \qquad (1\text{-}9)$$

and for n >2

$$\frac{\theta_n}{\theta_{n-1}} = \frac{p}{t_0/(1+k_R e^{cn})+1+p} = \alpha_n \qquad (1\text{-}10)$$

The surface fractions of alkyl chains with carbon number n can oe determined by successive calculation of the chain growth parameter with increasing carbon number:

$$\frac{\theta_n}{\theta_1} = \prod_{i=2}^{n} \alpha_i = \alpha_2\ \alpha_3 \ldots\ldots\ \alpha_n \qquad (1\text{-}11)$$

Also the molar selectivity of the various components m_i could be calculated by the following equations:

The molar selectivities for paraffins is:

$$m_{C_nH_{2n+2}} = \theta_1 \prod_{i=2}^{n} \alpha_i \qquad (1\text{-}12)$$

And the molar selectivities for olefins is:

$$m_{C_nH_{2n}} = \frac{t_0}{1+k_R e^{cn}}\ \theta_1 \prod_{i=2}^{n} \alpha_i \qquad (1\text{-}13)$$

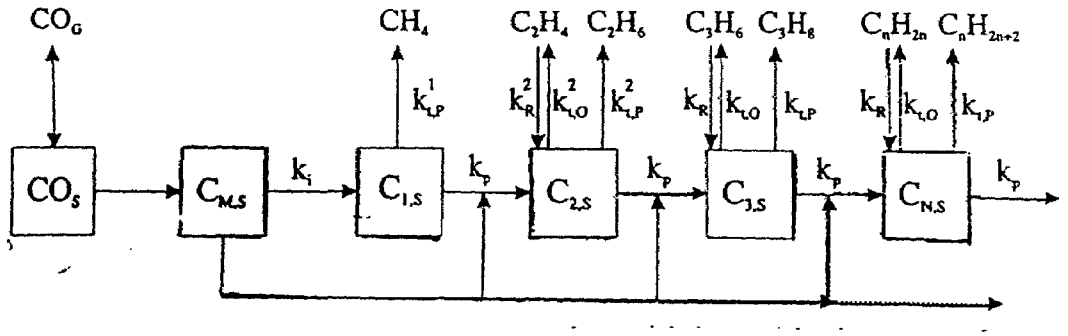

Figure 1.7 Reaction network α-Olefin Readsorption Product Distribution Model.

The model reduces to ASF model when k_R^2 and $k_R = 0$

The molar selectivities of the C_1 and C_2 products are calculated differently:

$$m_{CH_4} = t_p^1 \theta_1 \quad (1\text{-}14)$$

$$m_{C_2H_6} = t_p^2 \theta_2 = t_p^2 \alpha_2 \theta_1 \quad (1\text{-}15)$$

$$m_{C_2H_4} = \frac{t_0^2}{1+k_R^2} \theta_2 \quad (1\text{-}16)$$

The optimization constraint for the selectivities is:

$$\sum_i^n m_i = 1 \quad (1\text{-}17)$$

This model reduces to the ASF distribution model when olefins cannot adsorb i.e $k_R = 0$. The α-olefin readsorption product distribution model (ORPDM) accounts for the chain-length dependent readsorption of olefins on FT sites. The readsorption step depends on carbon number, resulting in a net decrease of the termination to olefins. α_n increases with increasing chain length until no olefins are formed. At high carbon numbers, the chain growth parameter, α_n, approaches a maximum constant value of α_∞ = p / (1+p). The increased readsorption of long-chain olefins results in a decreasing olefin/paraffin ratio with chain length. The number of parameters in model ORPDM is equal to 7: p, t_0, k_R, c, t_p^1, t_p^2 and k_R^2. Simultaneous optimization of these parameters showed four parameters to be independent of the experimental conditions. The average values of these parameters are shown in **Table 1.6 [Gerard vander-laan and Beennacker 2000]**

The model parameters p, t_0 ,k_R of model ORPDM is pseudo kinetic rate constants, incorporating true kinetic rate constants, surface concentrations of intermediates, hydrogen and vacant sites. Therefore, the model parameters vary with the adjusted process variables, P_{CO}, P_{H_2}, and space velocity. The effect of process variables on the model parameters is shown in **Table 1.7.**

Table 1.6 Optimized model parameters for ORPDM at 523 K that are independent of $\phi_{V,0}$, P, H_2 / CO ratio [Van der-Laan et al.,1999]

Model parameters	Value
t_p^1	6.5
t_p^2	1.7
k_R^2	(17.6) k_R e^{2c}
c	0.35

Table 1-7 Effect of process variables on model parameters [Van der-Laan et al., 1999]

parameter	Power law
P	14 $P_{H_2}^{-0.26}$ $P_{CO}^{0.40}$
t_0	3.71 $P_{H_2}^{-0.5}$
k_R	$8*10^{-5}$ $\frac{P_{H_2}^{1.2} P_{CO}^{-0.47}}{\phi_{V,0} / w}$

Pressures in MPa, space velocity $\phi_{V,0} / w$ in Nm^3/kg_{cat} .s

1-2-Slurry Bubble Column Reactor; General Design and Hydrodynamics

1-2-1-Slurry Phase Reactor (SPR)

Slurry phase bubble columns are receiving much attention as the favorable reactors for F-T synthesis based on natural gas because of their high capacity. They have been chosen by the big F-T developers Exxon Mobil and Sasol where cobalt based catalyst is employed.

The design of a general three phase reacting system (gas-liquid-solid reactors) is complex because of simultaneous occurrence of chemical reactions and transport processes, which mutually interact. The FT slurry reactor is a complicated system whose adequate understanding requires resolution of features involving FT chemistry and kinetics, hydrodynamics and transport processes in relation to mass and energy. A slurry reactor is typically a cylindrical column with length/ diameter ratio (aspect ratio) ranging from 5 to 10 **[Shah et al., 1982]**. Syn-gas is continuously introduced at the bottom of the reactor through a distributor device such as a porous plate, orifice jet, or sparger ring **[Saterfieled and Huff, 1980 and Deckwer et al, 1981].**

The gas bubbles that form at the distributor rise through the slurry and provide the agitation necessary to maintain the catalyst particles in uniform suspension. The particle size of the commonly used catalyst is typically less than 50 μm **[Shah et al., 1982]**.

The unconverted synthesis gas and volatile reaction products exit from the top of the reactor after residence time not exceeding several minutes duration. The liquid product is withdrawn from the reactor on either a batch or continuous basis. The FT slurry reactors are typically operated at temperatures between 493 K and 573 K.

The equilibrium size of bubbles, gas holdup, specific gas-liquid surface area, and the mass transfer coefficient are important parameters establishing the degree of chemical conversion in a bubble column reactor. Bubble velocity and its residence time in the column are controlled by the properties of the liquid or slurry phase in addition to its size and configuration. These phase properties in turn are also influenced by the operating conditions such as temperature, pressure, catalyst particle size and size range, and slurry concentration. The configuration of the internal heat exchanger also controls the equilibrium bubble size and liquid mixing. Thus, it is obvious that the selection of all these interacting design parameters for a real reacting system

is a difficult task, and in the next section all the hydrodynamic theory and experimental experience are pooled to help accomplish this goal.

The procedure for designing a bubble column reactor [BCR] should start with an exact definition of the requirements, i.e. the required production level, the yields and selectivities. These quantities and the special type of reaction under consideration permits a first choice of the so called **adjustable** operational conditions which include phase velocities, temperature, pressure, direction of the flows. In addition, process data are required. They comprise physical properties of the reaction mixture and its components [densities, viscosities, heat and mass transfer, diffusivities, surface tension], phase equilibrium data (above all solubilities) as well as the chemical parameters. The latter are particularly important, as they include kinetic and thermodynamic (heat of reaction) information **[Deckwer et al., 1981].**

In multiphase reactor design hydrodynamic properties constitute another group of important parameters. These are more or less "**non adjustable**" or "self adjusting" quantities dependent on the chosen reactor geometry, the adjustable operational conditions as well as the process data. Under this notation we summarize the phase holdups, the interfacial areas, the heat and mass transfer properties and the dispersion coefficients.

All these quantities, i.e. the geometry, the process data, the adjustable and non adjustable parameters, are then introduced in the reactor model equations derived on the basis of the physical and chemical phenomena which are suspected to take place within the reactor. Usually the model equations have to be solved numerically as they contain strong nonlinearities (temperature dependency of reaction rates and solubilities, phase flow variation).

The general scheme outlined in **figure (1-8)** represents the requirements for a reactor model. The use of models and model simulations are extremely useful in all design and scale up considerations, mathematical methods to solve model equations of any degree of complexity are available, and fast numerical techniques have been developed **[Deckwer et al., 1981].**

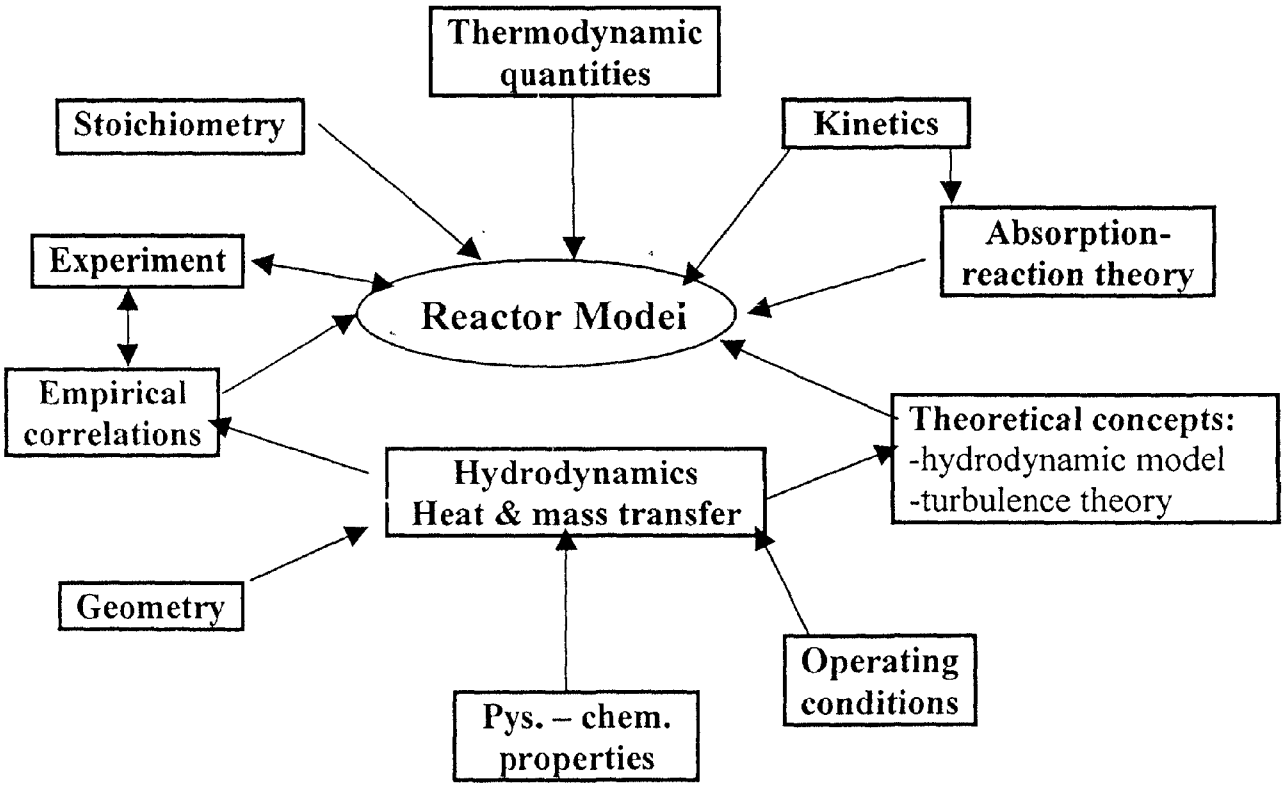

Figure (1-8) Phenomena Involved in Modeling Bubble Column Slurry Reactor

1-2-2-Hydrodynamics

In the following sections of this chapter the various aspects of hydrodynamics and important design parameters will be presented. This includes the following topics:

1-2-2-1-Flow Regime

1-2-2-2-Bubble Dynamics

1-2-2-3-Gas Holdup

1-2-2-4-Gas-Liquid Interfacial Area

1-2-2-5-Mass Transfer Coefficients

1-volumetric gas-liquid mass transfer coefficient, k_La

2-liquid side mass transfer coefficient, k_L

3-gas side mass transfer coefficient, k_G

4-liquid-solid mass transfer coefficient, k_S

1-2-2-6- Back mixing or dispersion coefficients

1-gas-phase dispersion, D_G

2- liquid-phase dispersion, D_L

3- solid-phase dispersion, D_s

1-2-2-7- Heat transfer, h

1-2-2-1- Flow Regime

In bubble column reactors the hydrodynamics, transport and mixing properties such as pressure drop, holdup of various phases, fluid-fluid interfacial areas and inter-phase mass and heat transfer coefficients depend on the prevailing flow regime **[Shah et al., 1982]**. These can be categorized as:

1-Homogenous Regime or Bubbly Flow:

This regime is characterized by almost uniformly sized bubbles with equal radial distribution. This regime occurs if the superficial velocity is less than 0.05 m/s and the rise velocity of the bubbles lie between 0.18 - 0.3 m/s. The bubble size distribution is narrow and a roughly uniform bubble size; generally in the range 1 - 7 mm is found **[Shah et al., 1982]**.

2-Heterogeneous or Churn -Turbulent Regime:

When the superficial gas velocity U_G reaches the value U_{Trans}, coalescence of the bubbles takes place to produce the first fast rising "large bubbles". This changes the hydrodynamic picture dramatically. The hydrodynamic regime is commonly referred to as the heterogeneous flow regime.

In the heterogeneous regime, small bubbles combine in clusters to form large bubbles in the size range 20-70 mm. The large bubbles are non spherical and of

varying form with very mobile and flexible surfaces, for instance, spherical caps **[Deckwer et al., 1981].** They travel up through the column at high velocities (1-2 m/s) in a more or less plug flow manner. These large bubbles have the effect of churning up the liquid phase. The large bubbles are mainly responsible for the throughput of gas through the reactor at high velocities. Small bubbles, which co-exist with large bubbles in the churn-turbulent regime, are "entrained" in the liquid phase, and as a good approximation have the same back mixing characteristics of the liquid phase. The heterogeneous or churn-turbulent regime is most commonly encountered in industrial bubble columns where the two bubble classes with significantly differing sizes and rise velocities can be observed **[Krishna and Sie, 2000].** However the homogeneous flow regime is encountered as well, particularly in pressurized BCSRs **[Deckwer and Schumpe, 1993].**

3-Slug Flow:

In small diameter columns at high gas flow rates, large bubbles are stabilized by the column wall leading to the formation of bubble slugs. Bubble slugs can be observed in columns of diameters up to 0.15 m **[Shah et al., 1982].**

The type of sparger used, physico-chemical properties of liquid, and the liquid velocity can affect the transition between the flow regimes **[Shah et al., 1982].** The dependence of flow regime on column diameter and gas velocity can be roughly estimated from **figure (1-9).**

1-2-2-2-Bubble Dynamics

Bubble size, bubble rise velocity, bubble size distribution and liquid and bubble velocity profiles have a direct bearing on the performance of bubble columns. The majority of bubble column reactors used in industry are operated at high pressures. Studied systems showed that up to pressures of 1.6 MPa , there is no effect on the gas holdup and mean bubble diameter if the gas velocity is corrected to take into account the pressure in the column **[Shah et al., 1982].**

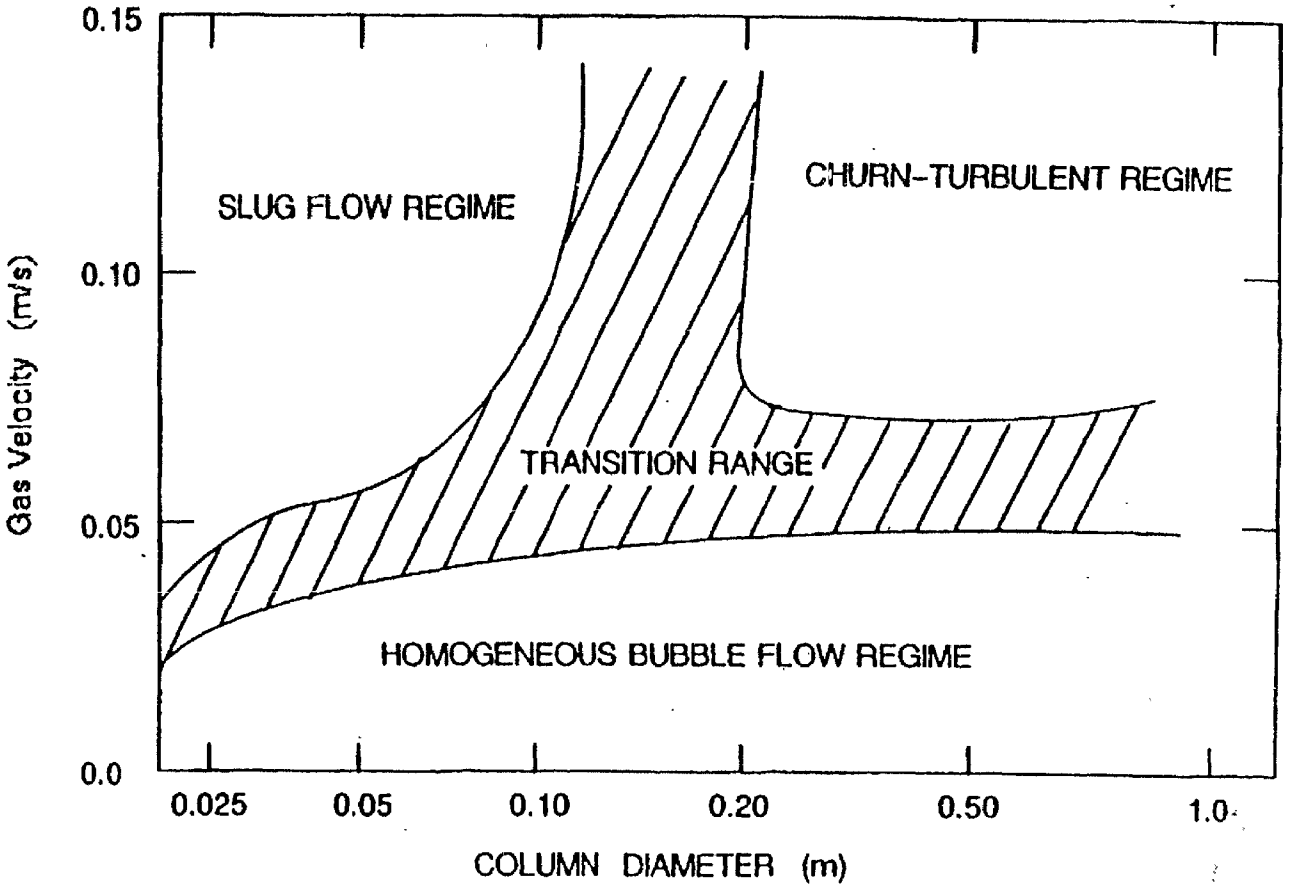

Figure 1-9 Types of Flow Regimes [Shah et al., 1982].

The mean rise velocity of the bubbles in a bubble swarm is equivalent to the interstitial gas velocity V_G^* which follows from the superfacial gas velocity U_G :

$$V_G^* = U_G / \varepsilon_G.$$

In the bubbly flow regime the rise velocity may vary from 0.03 to 0.2 m/s. If the flow is churn-turbulent, rise velocities are considerably higher $\geq$ 0.8 m/s. The transition from bubbly to churn-turbulent flow is usually accompanied by a sharp increase in V_G^*. **[Shah et al., 1982]**.

1-2-2-3-Gas Holdup

Gas holdup is one of the most important parameters characterizing the hydrodynamics of bubble columns. It can be defined as the percentage by volume of the gas in the two or three phase mixture in the column. It has two fold applications. On one hand, the gas holdup in two phase systems gives the volume fraction of the phases present in the reactor and hence their residence times. On the other hand, the gas holdup in conjunction with the knowledge of mean bubble diameter d_{vs}, allows the determination of the interfacial area and thus leads to the mass transfer rates between the gas and liquid phase. Gas holdup depends mainly on the superficial gas velocity and often is very sensitive to the physical properties of the liquid and gas **[Shah et al., 1982]**. The relative gas holdup varies locally in axial and radial direction. It largely depends on the flow regime, if it is homogeneous (bubbly) or heterogeneous (churn-turbulent).The dependence of the gas holdup on gas velocity is generally of the form, $\varepsilon_G \quad \alpha \quad U_G^n$

The value of the exponent, n, depends on the flow regime. In homogeneous bubbly flow regime the value of n varies from 0.7 to 1.2, while for churn-turbulent or the transition regime, the effect of U_G is less pronounced and the exponent n takes values from 0.4 to 0.7.

A large number of correlations for gas holdup have been proposed in the literature **[Shah et al., 1982]**; however, the large scatter in the reported data does not allow a single correlation. The presence of solids does not affect the gas holdup significantly at high gas velocities > 0.1 m/s **[Shah et al., 1982]**.

1-Factors Affecting Gas Holdup

i-Sparger and column geometry.

The gas hold up is virtually independent of column dimensions and sparger layout [for low as well as high pressures] provided the following three criteria are fulfilled **[Wilkinson, et al., 1992]:**

1- The column diameter has to be larger than 0.15 m.
2- The column height to diameter ratio has to be in excess of 5.

3- The hole diameter of the sparger has to be larger than 1-2 mm.

ii- Gas Density

Wilkinson and Dierendonck, [1990] have demonstrated that a higher gas density increases the rate of bubble breakup especially for large bubbles. As a result, at high pressure mainly small bubbles occur in homogeneous bubble flow, until for very high gas holdup the transition to the churn turbulent regime occurs because coalescence then becomes so important that larger bubbles are formed **[Wilkinson et al., 1992].**

iii- Liquid Properties

Liquid properties such as viscosity and surface tension have an influence on the regime transition (and gas holdup). A higher liquid viscosity promotes coalescence of large bubbles. Consequently, large bubbles occur especially in bubble columns with high viscosity liquids. Furthermore, because of the high-rise velocity of these large bubbles, the gas holdup in viscous liquids is expected to be low, whereas the transition to the churn turbulent regime occurs at very low gas velocity. The surface tension also has a pronounced influence on bubble break up (and thus holdup). The occurrence of large bubbles is minimal due to bubble break up especially in those liquids that combine a low surface tension with a low viscosity. As a result, relatively high gas holdup values are to be expected for such liquids, whereas the transition to the churn-turbulent regime due to the formation of large bubbles is delayed to relatively high gas holdup values **[Wilkinson et al., 1992]**

iv- Temperature

It has been demonstrated that a temperature increase in general leads to a higher gas holdup. A change in temperature can have an influence on gas holdup, due to the influence of temperature on the physical properties of the liquid, and on the vapor pressure. Both the surface tension and the liquid viscosity decrease if the temperature is increased, and this will lead to a higher gas holdup **[Wilkinson et al., 1992].**

v- Suspended Solids

From many publications it has become clear that the addition of solids to a bubble column will lead to a small decrease in gas holdup **(Reilly et al., 1986)** and the formation of large bubbles an exception occurs for very small particles (0 – 100) μm at low weight fractions (< 4%) **[Wilkinson et al., 1992].**

vi- Liquid Velocity

The liquid velocity in a bubble column is usually low, and consequently its influence on gas holdup is often claimed to be negligible. In principal, however, liquid flowing co currently up ward will lower gas holdup, while a counter current liquid flow will increase gas holdup **[Wilkinson et al., 1992].**

Correlations for calculating the gas holdup

Shah et al., [1982] listed 14 different correlations for gas holdup in two- and three phase systems together with the system employed and the range of operating parameters, only a few one are based on numerous experimented data e.g.

Akita and Yoshida, [1973]

$$\frac{\varepsilon_G}{(1-\varepsilon_G)^4}=0.2\left[\frac{D_R^2\,\rho_L\,G}{\sigma}\right]^{1/8}\left[\frac{g\,D_R^3\,\rho_L^2}{\mu_L^2}\right]^{1/12}\left[\frac{U_G}{\sqrt{gD_R}}\right] \qquad \textbf{(1-18)}$$

And Hikita et al. [1980]

$$\varepsilon_G = 0.672\left[\frac{U_G\,\mu_L}{\sigma}\right]^{0.578}\left[\frac{(\mu_L^4 g)}{\rho_L\sigma^3}\right]^{-0.131}\left[\frac{\rho_G}{\rho_L}\right]^{0.062}\left[\frac{\mu_G}{\mu_L}\right]^{0.107} \qquad \textbf{(1-19)}$$

Wilkinson et al., [1992] listed some other equations incorporating the gas phase properties and accounts for the influence of gas velocity on gas holdup in the churn-turbulent regime by assuming that gas holdup increases less than linear proportionally [$\varepsilon_G \approx U_G^{0.4-0.6}$ or $\frac{\varepsilon_G}{1-\varepsilon_G} \approx U_G^{0.6-0.9}$] to the superficial gas velocity U_G,

Hammer et al., [1984]

$$\frac{\varepsilon_G}{1-\varepsilon_G} = 0.4\ U_G^{0.87}\ \rho_L^{0.1}\ \rho_G^{0.17}\ \sigma^{-0.06}\ \mu_L^{-0.21}\ g^{-0.27} \qquad \textbf{(1-20)}$$

Idogawa et al., [1985]

$$\varepsilon_G = I/(I+1) \quad I = 1.44\ U_G^{0.58}\ \rho_G^{0.12}\ (\sigma)^{(-0.16\exp(-P))} \qquad \textbf{(1-21)}$$

P pressure in Mpa ; σ surface tension in mN/m

Reilly et al., [1986]

$$\varepsilon_G = 296\ U_G^{0.44}\ \rho_L^{-0.98}\ \rho_G^{0.19}\ \sigma^{-0.16} + 009 \qquad \textbf{(1-22)}$$

Idogawa et al., [1987]

$$\frac{\varepsilon_G}{1-\varepsilon_G} = 0.059\ U_G^{0.8}\ \rho_G^{0.17}\left[\frac{\sigma}{72}\right]^{-0.22\exp(-P)} \qquad \textbf{(1-23)}$$

P: pres in Mpa ; σ : surface tension in mN/m and U_G : in cm/s

In the heterogeneous flow **Krishna et al., [1991] and Wilkinson, [1991] and Krishna and Sie, [2000] assume** that the small bubbles holdup is constant and equal to that at the end of the homogeneous flow regime (ε_{trans}). Increasing the gas velocity beyond the transition velocity U_{trans} from homogeneous to heterogeneous flow increases only the large bubble holdup and the following relations are assumed to apply:

Krishna et al. [1991]

$$\varepsilon_{G\,\mathrm{hom}} = 4\,U_G$$

$$\varepsilon_{LB} = A\,(U_G - U_{trans})^n \qquad U_G \geq U_{trans}$$

$$\varepsilon_{hetro} = \varepsilon_{trans} + A\,(U_G - U_{trans})^n \qquad \textbf{(1-24)}$$

$$\varepsilon_{trans} = 4\,U_{trans}$$

with $A=1$, $n=0.8$ and U_{trans} taken from experiments could describe gas holdup data up to 0.5 with striking agreement.[**Krishna et al. 1991**

Wilkinson, [1991]

$$\varepsilon_G = U_G / V_{DF} \qquad U_G \le U_{trans}$$

$$\varepsilon_G = \frac{U_{trans}}{V_{DF}} + \frac{U_G - U_{trans}}{V_{LB}} \qquad U_G > U_{trans}$$

$$\frac{V_{DF}\,\mu_L}{\sigma} = 2.25 \left[\frac{\sigma^3 \rho_L}{g\,\mu_L^4}\right]^{-.273} \left[\frac{\rho_L}{\rho_G}\right]^{0.03}$$

$$\frac{V_{LB}\,\mu_L}{\sigma} = \frac{V_{DF}\,\mu_L}{\sigma} + 2.4 \left[\frac{\mu_L (U_G - U_{trans})}{\sigma}\right]^{0.757} \left[\frac{\sigma^3 \rho_L}{g\mu_L^4}\right]^{-0.077} \left[\frac{\rho_L}{\rho_G}\right]^{.077} \frac{U_{trans}}{V_{DF}}$$

$$\varepsilon_{trans} = 0.5 \exp(-193\ \rho_G^{-0.61} \mu_L^{0.5}\ \sigma^{0.11}) \qquad \textbf{(1-25)}$$

Krishna and Sie, [2000] further assumed that the rise velocity of small bubbles will increase with increased solids holdup due to enhanced coalescence according to :

$$V_{DF} = V_0 \left(1 + 0.8\, \varepsilon_p / V_0\right)$$

$$\varepsilon_{DF} = \varepsilon_{DO} \left(\frac{\rho_G}{\rho_{GO}}\right)^{0.48} \left(1 - 0.7\, \varepsilon_p / \varepsilon_{DO}\right)$$

$$U_{DF} = \varepsilon_{DF}\, V_{DF}$$

$$U_{LB} = U_G - U_{DF}$$

$$\varepsilon_{LB} = 0.3 \quad U_{LB}^{0.58} \left(\frac{\rho_G}{\rho_{GO}}\right)^{0.5}$$

$$\varepsilon_G = \varepsilon_{LB} + \varepsilon_{DF} \left(1 - \varepsilon_{LB}\right) \qquad \textbf{(1-26)}$$

With: $V_0 = 0.095$ m/s ρ_{G0}=1.3 $\varepsilon_{D0} = 0.27$ D>1m ε_P>0.16

1-2-2-4-Gas-Liquid interfacial area, *a*

The gas-liquid interfacial area is an important design variable, which depends on the geometry of apparatus, the operating conditions and the physical properties of liquid media. The influence of column diameter on the interfacial area vanishes at

large column diameters, say $D_R > 0.15$ m. The methods used to measure the interfacial area in gas-liquid dispersion fall into two main categories; namely, physical and chemical methods. The physical methods determine the size of the bubbles. If a chemical method is used to determine *a,* a suitable reaction is applied. Interfacial areas determined from the physical and chemical methods may differ by more than 100%. The specific interfacial area *a*, can be calculated from the gas hold up and volume–to surface mean bubble diameter d_{vs}, **[Shah et al., 1982]** as: -

$$a = 6\,\varepsilon_G / d_{VS}$$

1-2-2-5-Mass Transfer Coefficients

1-Volumetric gas-liquid mass transfer coefficient, $k_L a$

The interfacial area a and the liquid volumetric mass transfer coefficient $k_L a$ are considered the most important design parameters for bubble column reactors **[Wilkinson et al., 1992].**

Volumetric mass transfer coefficients depend on the gas velocity, the sparger design and are sensitive to physico-chemical properties particularly those, which promote or prevent coalescence. Further more $k_L a$ may vary spatially. Sometimes larger $k_L a$ values are observed in the immediate vicinity of the sparger than in the bulk region. In addition, the column diameter has some influence if it is small <0.15 m. In the three phase bubble column reactors, $k_L a$ can be affected by the presence of solids. Investigations of various authors indicate that the degree of influence of suspended particles on $k_L a$ depends on the particle concentration, the particle size, the liquid-solid density difference, the geometrical sizes and the operating conditions of the reactor [*i.e.* gas, liquid velocities].

For the typical operating conditions prevailing in the Fischer-Tropsch synthesis in slurry phase, **Deckwer et al. [1980]** have shown that the presence of solid particles (diameter less than $50\,\mu m$, concentration of solids (<16 % wt) gives a negligible effect on $k_L a$. Also it is obvious that both the increase in gas holdup and the

decrease the bubble size with increasing pressure lead to a higher interfacial area, a and $k_L a$

Correlations for calculating the volumetric gas-liquid mass transfer coefficient, $k_L a$:

Akita and Yoshida[1973]

$$\frac{k_L a D_R^2}{D_v} = 0.6 \left[\frac{\mu_L}{\rho_L D_V}\right]^{0.5} \left[\frac{g D_R^2 \rho_L}{\sigma}\right]^{0.62} \left[\frac{g D_R^3 \rho_L}{\mu_L^2}\right]^{0.31} (\varepsilon_G)^{1.1} \qquad \textbf{(1-27)}$$

The dependency of $k_L a$ on D_R exists, if at all, only for small diameter and for D_R => 0.6 m it is recommended to use D_R=0.6 m

Hikita et al., [1981]

$$\frac{k_l a U_G}{G} = 14.9 \left[\frac{U_G \mu_L}{\sigma}\right]^{1.76} \left[\frac{\mu_L^4 g}{\rho_L \sigma^3}\right]^{-0.248} \left[\frac{\mu_G}{\mu_L}\right]^{0.243} \left[\frac{\mu_L}{\rho_L D_V}\right]^{-0.604} \qquad \textbf{(1-28)}$$

Vemeer and Krishna, [1981]

The $k_L a$ of large and small bubbles is obtained from the relations :-

$$k_L a_{\ small} = \varepsilon_{DF} \left(D_V / D_{VO}\right)^{0.5} \quad : \quad k_L a_{large} = 0.5\, \varepsilon_{LB} \left(D_V / D_{V0}\right)^{0.5} \qquad \textbf{(1-29)}$$

Deckwer et al., [1992] and Deckwer and Schumpe, [1993].

$$Sh = 0.6\, Sc^{0.5}\, Bo^{0.62}\, Ga^{0.31}\, \varepsilon_G^{1.1} \qquad \textbf{(1-30)}$$

With $D_R = 0.6$ m

Ozturk et al., [1987]

$$\left[\frac{k_L a D_B^2}{D_V}\right] = 0.62 \left[\frac{\mu_L}{\rho_L D_V}\right]^{0.5} \left[\frac{g \rho_L D_B^2}{\sigma}\right]^{0.33} \left[\frac{g \rho_L^2 D_B^3}{\mu_L^2}\right]^{0.29} \left[\frac{U_G}{\sqrt{g D_B}}\right]^{0.68} \left[\frac{\rho_G}{\rho_L}\right]^{0.04} \qquad \textbf{(1-31)}$$

With D_B = 0.003 m

Wilkinson [1991]

$$\frac{(k_L a)_{\rho_{G2}}}{(k_L a)_{\rho_{G1}}} = \left[\frac{(\varepsilon_G)_{\rho_{G2}}}{(\varepsilon_G)_{\rho_{G1}}}\right]^n \qquad (1\text{-}32)$$

With n= 1.0 - 1.2

2-Liquid side mass transfer coefficients, k_L

For mass transfer processes accompanied by slow chemical reaction it is not required to separate the volumetric mass transfer coefficient into its individual quantities, *i.e.* k_L and a. If the reaction in the liquid is fast and instantaneous the reaction take place within the liquid film and knowledge of k_L is required to calculate the enhancement factors **[Deckwer, et al., 1981]**.

A number of empirical and theoretical equations for evaluating k_L are available in the literature. However, the predictions of various correlations scatter considerably. As a rule of thumb it can generally be assumed that for gas in liquid dispersion k_L varies from 0.01 to 0.03 cm/s **[Deckwer, et al., 1981]**.

3-Gas side mass transfer coefficient, k_G

Gas side resistance to mass transfer becomes important during the absorption of highly soluble lean gas accompanied by instantaneous and irreversible chemical reaction **[Shah et al., 1982]**.

The gas phase mass transfer coefficient k_G, however, decrease with increasing pressure due to the fact that the gas diffusion coefficient is inversely proportional to pressure, $k_G = D_G^n = p^{-n}$

The value of n in this equation is usually found to be close to 0.5. As a consequence, the favorable increase in the interfacial area a and $k_L a$ due to a higher pressure will in some cases (especially for soluble gases) be limited by the decrease in the gas-phase mass transfer coefficient at higher pressures. Finally, it is also possible that the performance of high-pressure bubble columns limited for relatively slow reactions, because for slow reactions a decrease of the liquid-phase reaction volume (as a result of the higher gas holdup at high pressure) can lead to a lower overall reaction rate **[Wilkinson et al., 1992]**

4-Liquid-solid mass transfer coefficients, k_S

In the three phases bubble columns slurry reactors, the mass transfer from bulk liquid to the solid surface can play an important role in the overall apparent reaction rate. The equation by **Deckwer, et al., [1981]** was recommended by **[Shah et al., 1982]** for the calculation of liquid-solid mass transfer since it covers a wide range of the experimental parameters.

$$Sh^* = 2.0 + 0.545\, Sc^{1/3} \left[\frac{e\ d_p^4}{v^3} \right]^{0.264} \qquad \textbf{(1-33)}$$

$$Sc = \frac{\mu_L}{\rho_L\ D_V}$$

1-2-2-6-Backmixing or Dispersion coefficients

A useful description of mixing in bubble columns is provided by the dispersion model. The global mixing effects are generally characterized by the dispersion coefficients D_L, D_G of the two phases, which are defined in analogy to Fick's law for diffusive transport **[Deckwer, et al., 1981]**.

1-Gas phase dispersion (Gas mixing), D_G

Bubble column reactors are often modeled with neglect of gas phase mixing. This is only permitted for tall bench-scale reactors where the Bodenstein numbers $(Bo_G = U_G.\ L\ /\ (\varepsilon_G\ D_G)$ with D_G calculated from the available correlations are high, say $Bo_G \geq 10$. For large diameter columns the plug flow assumption is no more justified. Mixing of the gas phase of BCRs is considerable and is attributed to different bubble rise velocities, bubble coalescence and break up and circulation of bubbles. All the various phenomena are lumped into the gas phase axial dispersion coefficient D_G and axial dispersion model is used to describe globally gas phase mixing. In contrast to the liquid phase, gas phase dispersion largely affects bubble column reactor performance.

In spite of its importance, comparatively little work has been reported on gas phase dispersion. One reason may be that gas phase dispersion coefficients are relatively difficult to determine **[Deckwer and Schumpe, 1993]**.

Correlations for calculating the gas dispersion coefficient

Mangartz and Pilhofer [1980]

$$D_G = 50 D_R^{3/2} (U_G / \varepsilon_G)^3 \qquad \textbf{(1-34)}$$

at atmospheric conditions

Joshi [1982]

$$D_G = 110\, U_G^2\, D_R^2 / \varepsilon_G \qquad \textbf{(1-35)}$$

Wachi and Nojima [1990]

$$D_G = 20\, D_R^{3/2} \quad U_G \qquad \textbf{(1-36)}$$

2- Liquid phase dispersion, D_L

Mixing of the liquid phase in the bubble column reactor has to be attributed to various phenomena such as turbulent vortices, liquid entrainment in the wakes of rising bubbles, liquid circulation, radial exchange flows, etc. All these phenomena are obviously interrelated and are primarily dependent on the gas holdup structure, i.e. local holdup variations, bubble size and rise velocity distributions.

The dispersion coefficient of the liquid phase is dependent on the gas velocity and on the column diameter. The liquid flow, the type of gas sparger and the physico-chemical properties of the liquid like viscosity have little effect on the dispersion coefficient.

The various correlations described in the literature show dependencies of D_L on the diameter of reactor D_R, which range from $D_R^{1.0}$ to $D_R^{1.5}$ and on the gas velocities in the range of $U_G^{0.3}$ to $U_G^{2.0}$. **Rice et al. [1980]** attributed these large variations to the different flow regimes, they proposed that as

1- in chain bubbling $D_L \alpha U_G^{2.0}$ 2- in bubbling flow $D_L \alpha U_G^{1.0}$

3- in churn-turbulent flow $D_L \alpha U_G^{1/3}$ 4- in slug flow $D_L \alpha U_G^{0.0}$

The effect of liquid phase mixing on bubble column reactor performance is only minor and seemingly often overestimated. In many practical applications and reaction engineering estimates, the assumption of a backmixed liquid phase is justified. When using bubble columns as absorbers and reactors, the available space-time-yields are little affected by variations of liquid phase dispersion or circulation. Also, when evaluating mass transfer coefficients $k_L a$ for measured steady state liquid phase concentration profiles, $k_L a$ show little sensitivity to considerable variations of D_L **[Deckwer and Schumpe, 1993]**.

Correlations for calculating the liquid dispersion coefficient:-

Deckwer et al. [1980]

$$D_L = 2.7\, U_G^{0.3}\, D_R^{1.4} \qquad \textbf{(1-37)}$$

Deckwer and Shumpe [1993]

$$D_L = 0.35(U_G\, G)^{1/3}\, (D_R)^{4/3} \qquad \textbf{(1-38)}$$

Wilkinson [1991]

$$D_L \text{ (high pressure)} = D_L \text{ (atm)} \; \frac{\varepsilon_L \;\; atm}{\varepsilon_L \;\; high\ press} \qquad \textbf{(1-39)}$$

3- Solids phase dispersion, D_S

The physical properties of the liquid such as density and viscosity influence the value of the solids dispersion coefficient. Also it depends on the operating conditions of the column such as the gas velocity and the gas holdup. The particle diameter and its settling velocity also affect the solid dispersion coefficient (*Ds*).

It was found that the solids dispersion coefficient was larger for the baffled than for unbaffled column. The presence of baffles increased the intensity of solids mixing. The use of baffles in a slurry column in general provided a more uniform axial solids concentration distribution than an un-baffled column for otherwise identical operating conditions. The effect was more pronounced at lower gas velocities (< 0.1 m/s). This was attributed to increase mixing and reduced hindered

settling velocities when baffles were present in a bubble column. Also the ratio U_{ST}/Ds was proposed as measure of the uniformity of the axial concentration. A smaller U_{ST}/Ds value implied a more uniform profile **[Saxena et al., 1995]:**

Correlations for calculating the solid dispersion coefficient:-

O'Dowed et al. [1985] reported the following expression for the estimation U_{ST} for the baffled and unbaffled columns, respectively, on the basis of a regression analysis of their data

$$U_{ST} = 1.86\, U_G^{0.3}\, U_t^{0.8}\, \varepsilon_L^{3.5} \qquad \text{for baffled columns} \qquad (1\text{-}40)$$

$$U_{ST} = 1.69\; U_G^{0.23}\; U_t^{0.8}\; \varepsilon_L^{1.28} \qquad \text{for unbaffled columns} \qquad (1\text{-}41)$$

Also they suggested the following equations for the estimation of D_S

$$Pe_S = 7.4(Fr_G^6 / \mathrm{Re}_G)^{0.115} + 0.019\,\mathrm{Re}_S^{1.1} \qquad \text{for baffled columns} \qquad (1\text{-}42)$$

$$Pe_S = 7.7(Fr_G^6 / \mathrm{Re}_G)^{0.098} + 0.019\,\mathrm{Re}_S^{1.1} \qquad \text{for unbaffled columns} \qquad (1\text{-}43)$$

where

$$Pe_S = U_G D_R / D_S \qquad 0.3 < Pe_S > 1.2 \qquad (1\text{-}44)$$

$$\mathrm{Re}_G = U_G D_R \rho_L / \mu_L \qquad 2100 < Re_G > 29000 \qquad (1\text{-}45)$$

$$Fr_G = U_G / (g\, D_R)^{1/2} \qquad 0.03 < Fr_G > 0.2 \qquad (1\text{-}46)$$

$$\mathrm{Re}_S = d_p\, \rho_L\, U_t / \mu_L \qquad 0.1 < Re_S > 5.6 \qquad (1\text{-}47)$$

1-2-2-7-Heat transfer, *h*

The heat transfer rate from the dispersion in the bubble column to either an immersed surface or the column wall is high due to the gas bubble induced vigorous mixing of the liquid or slurry phase. An internally placed cooling tube arrangement is the most efficient and economic alternative for removal of the heat of reaction from a slurry bubble column catalytic reactor.

The value of heat transfer coefficient, h, depends on the operating conditions such as superficial gas velocity, U_G; reactor temperature, T; operating pressure, P; thermo-physical and transport properties of the gas, liquid and solid phases, solid concentrations, particle size and size range and the configuration of the heat exchanger system.

There is a general consensus that h is independent of **column diameter** as long as it is greater than 10 cm for un-baffled configurations of the heat exchanger system. However, the design of the heat exchanger tube bundles is serious. The inter tube separation or pitch should be large enough not to hamper liquid mixing and movement by impeding the bubble velocity. On the other hand, control of the bubble diameter through tube pitch in the heat exchanger by limiting its growth will improve mass transfer by increasing the interfacial area per unit bubble volume. Thus optimum tube bundle configuration design for a slurry bubble column is a challenging industrial problem.

The **gas sparger** design has very little influence on h in the churn-turbulent flow regime but is crucial for operation in the bubbly-flow regime for gas velocities lower than about 5 cm/s.

There is near unanimous agreement concerning the qualitative dependence of h on U_G. Investigators found h to increase rapidly with an initial increase in U_G till about 0.14 or 0.16 m/s, and there after further increases in U_G produced very little influence on h values.

The influence of **temperature** on h has been found to increase with increases in temperature. This increase is brought about by the changes in the thermodynamic and transport properties of the liquid or slurry phase as the temperature is altered.

It was also found that h increased with an increase in **solid concentration** w_S for large particles for all types of liquid phases through an increase in ρ_{SL}, $C_{p,SL}$ and k_{SL}. For small particles the rheology of the pseudo-homogeneous slurry phase would play an important role and h may increase as well as decrease depending

upon the value of μ_L *and* μ_{SL}. Viscosity plays an important role through its influence on bubble diameter **(Saxena et al., 1995)**.

The heat transfer coefficients in bubble columns are many times larger than that for single-phase flow. **Deckwer et al., [1980]** pointed that the radial component of the liquid velocity, which is induced by the rising bubble is responsible for the high heat transfer coefficients in bubble columns and presented a theoretical heat transfer model by combining the surface renewal model of mass transfer with Kolmogoroff's theory of isotropic turbulence. The final result in dimensionless form (when U_G <= 0.1) can be expressed as,

$$St = 0.1(\mathrm{Re}\ Fr\ \mathrm{Pr}^2)^{-0.25} \qquad \text{or} \qquad St = \frac{h}{\rho_{SL}\, C_{P,SL}\, U_G} \tag{1-48}$$

with

$$\mathrm{Re} = \frac{\rho_{SL} d_P}{\mu_{SL}} \qquad Fr = \frac{U_G^2}{g\, d_P}$$

$$\mathrm{Pr} = \frac{C_{P,SL}\mu_{SL}}{\lambda_{SL}}$$

further

$$C_{p,\,SL} = W_S C_{p,\,S} + W_L C_{p,\,L}$$

$$\lambda_{SL} = k_L \frac{2\lambda_L + \lambda_S - 2\phi_S(\lambda_L - \lambda_S)}{2\lambda_L + \lambda_S - \phi_S(\lambda_L - \lambda_S)} \quad \text{and}$$

$$\mu_{SL} = \mu_L(1 + 4.5\varepsilon_P)$$
$$\rho_{SL} = \varepsilon_P \rho_P + (1 - \varepsilon_P)\rho_L \tag{1-49}$$

1-3-Mathematical Models for Fischer-Tropsch Synthesis in Slurry Reactors.

The Fischer-Tropsch slurry reactor is a multiphase system of solid catalyst, liquid products, and gas-phase reactants. These reactants must diffuse through the liquid-phase to the catalyst surface in order for the Fischer-Tropsch synthesis to occur. **[Saxena, 1995]**

Mathematical models for F-T synthesis in slurry reactors have been developed by different groups of workers. These are **[Calderbank et al., 1963; Satterfield and Huff, 1980; Deckwer and coworkers, 1981 and 1982; Buker 1983 and Stern et al., 1983, 1985].** The differences in the models arise from the varying patterns assumed to describe the mixing in different phases **[Saxena, 1986] see table (1-8).**

The general approach in modeling the Fischer-Tropsch slurry reactor is to consider the specific mass transfer and kinetic rate processes that are taking place. In the slurry, the maximum possible concentrations of CO and H_2 are dictated by Henry's law. These concentrations are maintained at the gas-slurry interface, where the two phases are commonly assumed to be in equilibrium with each other. At the catalyst surface, CO and H_2 are being removed continuously from the slurry by chemical reaction. Therefore, in the general case, concentration gradients for CO and H_2 will exist between the gas-slurry interface and the catalyst surface, providing the necessary driving force for additional reactants to enter in the slurry phase. The magnitude of these gradients will be dependent on the relative rates of mass transfer and chemical reaction. Due to the reaction stoichiometry and difference in the rates of diffusion for CO and H_2, the H_2/CO ratio at the catalyst surface will, in general, be different from the corresponding ratio in the inlet gas or even at the gas-liquid interface at the same axial position in the reactor.

Table 1-8 Comparison of reaction engineering models for the Fischer-Tropsch synthesis in slurry bubble column reactors.

Reference	Gas phase	Liquid phase	Catalyst distribution	Energy balance	components
Calderbank et al. [1963]	PF	PF	Uniform	isothermal	H_2
Satterfield and Huff [1980]	PF	PM	Uniform	isothermal	H_2
Deckwer et al. [1981]	PF	PM	Uniform	isothermal	H_2
Deckwer et al. [1982]	AD	AD	non-uniform	non isothermal	H_2
Bukur [1983]	PF	PF, PM	uniform	isothermal	H_2
Stern et al. [1983]	PF	PM	Uniform	isothermal	H_2, CO, CO_2, H_2O, CH_4, C_5H_{10}
Kuo [1983]	PF	PM ,PF ,AD	non-uniform	isothermal	H_2
Kuo [1983]	PF	PF	non-uniform	isothermal	H_2, CO, CO_2, H_2O C_5H_{10}
Stenger and Satterfield [1985]	AD	AD	non-uniform	isothermal	H_2,CO,CO_2,H_2O, C_5H_{10}
Prakash and Bendale [1994]	AD	AD	non-uniform	isothermal	H_2,CO,CO_2,H_2O, C_{1-3}
Prakash [1994]	AD	AD	non-uniform	isothermal	H_2,CO,CO_2,H_2O, C_{1-3}
De Swart [1996][1]	AD	AD	non-uniform	non-isothermal	H_2
De Swart [1996][2]	PF	PM	uniform	isothermal	H_2
Mills et al. [1996]	AD	AD	non-uniform	non-isothermal	H_2
Inga and Morsi [1996]	PF	MC	uniform	isothermal	H_2, CO, H_2O
Krishna and Maretto [1998][2]	PF	PM	uniform	isothermal	H_2, CO
Van der Laan et al. [1999][2]	PF	PM	uniform	isothermal	H_2,CO, CO_2 ,H_2O,N_2, C_{1-100}

PF: plug flow, PM: perfectly mixed, MC: mixing cells, AD: axial dispersion
1 Heterogeneous flow regime: Large bubbles: PF, Small bubbles and liquid: AD
2 Heterogeneous flow regime: Large bubbles: PF, Small bubbles and liquid: PM

In the general case of the Fischer-Tropsch catalytic slurry reactor, the following specific transport and kinetic processes are commonly found to occur in series, as illustrated in **Fig. (1-10)** these are:

1) Diffusion of reactants through the gas film to the gas-liquid interface surrounding each bubble,
2) Diffusion of reactants through the liquid film surrounding each bubbles to the bulk liquid,
3) Diffusion of reactants through the liquid film surrounding each catalyst particle,
4) Diffusion of reactants through the catalyst pores to the inner catalyst surface, and
5) Reaction at the catalyst surface.

The mass transfer resistances offered by the gas film involving the transport of reactants from the bulk gas to the gas-liquid interface step1, and associated with the diffusion of reactants inside the catalyst pores to the active sites step 4 are generally considered to be negligible and have not been included in modeling the Fischer-Tropsch slurry reactors. However resistance associated with the transport of reactants across the gas-liquid interface is usually considered.

In all models, the resistances associated with the mixing and diffusion of the gaseous reactants in the bulk liquid phase is neglected.

It is also necessary in model development to consider the flow patterns for the gas phase, liquid phase and, solid catalyst. These flow patterns define the concentration profiles in the reactor and therefore influence the conversions predicted by the model

The simplest case is to assume that the catalyst is uniformly distributed throughout the slurry phase and to consider the gas phase and slurry to be either in plug flow or completely backmixed. Alternatively, the flow patterns may be modeled more realistically using the concept of axial dispersion. In

addition, the dispersion-sedimentation model may be applied to predict the extent of catalyst settling in the slurry reactor.

The mathematical models for F-T synthesis in slurry reactors as developed by the different groups of workers will be presented in the following section:

1-3-1-Mathematical Model of Caderbank et al. [1963]:

By considering the hydrogen balance, as shown in **figure (1-11), Calderbank et al. [1963]** formulated, at the steady state, the following relationship between the overall resistance, mass transfer resistance, and kinetic resistance by modeling the gas-liquid mass transfer and reaction at the catalyst surface as first–order rate processes that occur in series:

$$(RT / m'_{H_2})(1/k'_0) = [\varepsilon_G /(ak_{L,H_2})] + [\varepsilon_G /(k_c W\ k_{H_2})(1-\varepsilon_G)] \qquad (1\text{-}50)$$

The principal assumptions in the formulation of this model were as follows:

1- The Fischer-Tropsch slurry reactor is at the steady state, implying that thermodynamic equilibrium exists with respect to various state variables in each of the individual phases as well as at the interfaces of two different phases. The steady state operation also implies that there is no product accumulation in the reactor.

2- The gas phase and the slurry phase are in plug flow, and the catalyst particles are uniformly dispersed through out the slurry phase.

3- The gas phase obeys the ideal gas law.

4- The temperature and pressure are constant throughout the slurry reactor.

5- The F-T kinetics is first-order with respect to hydrogen concentration, and zero-order with respect to carbon monoxide concentration.

6- The overall reaction rate is controlled by the rate of mass transfer from the gas bubbles to the bulk liquid and the chemical reactions that occur at the catalyst surface.

7- The bubble size and gas hold up are constant throughout the reactor.

8- The concentrations of unconverted hydrogen and carbon monoxide in the liquid products exiting the reactor are negligible.

9- The liquid phase hydrogen concentration at the gas liquid interface obeys Henry's law.

10- The H_2/CO usage ratio remains constant and is the same as in the feed gas.

11- The volumetric gas flow rate $\dot{Q}$ is independent of reactor height and gas conversion.

12- The Fischer-Tropsch kinetics could be represented by a single reaction with the following stoichiometry:

$$1 \text{ reactants} \rightarrow \gamma \text{ products} \qquad (1\text{-}51)$$

Where γ stoichiometric coefficient, dimensionless

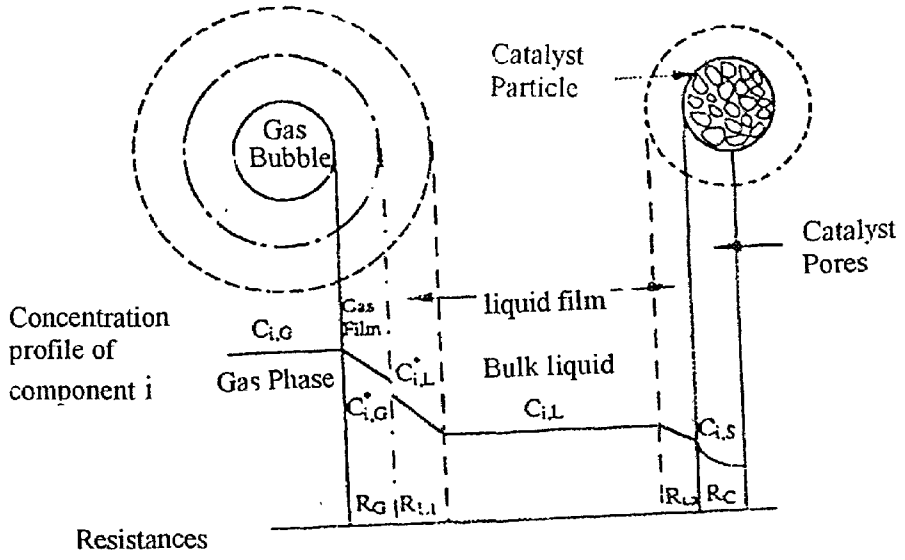

Figure (1-10) Concentration profile of component i and various resistances for mass transfer in a slurry bubble column

Calderbank et al. [1963] finally related the gas flow rate with the reactant conversion in the gas phase as:

$$k_0' \ \varepsilon_G \ V \ = \ Q \left[(1-\gamma)\, X^{e}_{H_2+CO} \ + \ \gamma \ Ln \ [1/(1-X^{e}_{H_2+CO})]\right] \qquad (1\text{-}52)$$

Equations (1-50) and (1-52) have been combined to obtain the following relation which was utilized by **[Calderbank et al., 1963]** to interpret their experimental data in which the gas-liquid interfacial area and the catalyst loading were varied over a range of conversions.

$$\frac{V}{\dot{Q}\, m''_{H_2}}\left(\frac{1}{(1-\gamma)\, X^{e}_{H_2+CO} + \gamma \ln[1/(1-X^{e}_{H_2+CO})]}\right) = \frac{1}{a\, k_{L,H_2}} + \frac{1}{(k_c\, W\, k_{H_2})(1-\varepsilon_G)} \qquad (1\text{-}53)$$

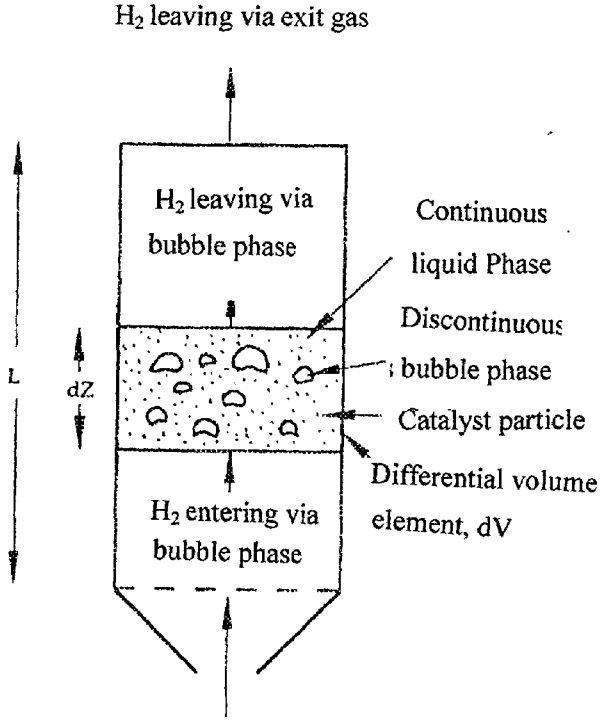

Fig (1-11) Schematic diagram of Fischer Tropsch slurry reactor H_2 mass balance

1-3-2-Mathematical model of Deckwer et al., (1981)

The Deckwer et al. [1981] model formulation is essentially based on the same assumptions as those of **[Calderbank et al., 1963] model.** However, **Deckwer et al. [1981]** considered arbitrary H_2/CO ratio values in the feed gas, which could be different from the stoichiometric or H_2/CO usage ratio values. This was accomplished by adopting the following reaction stoichiometry:

$$H_2 \quad + \quad U\,CO \rightarrow \quad \gamma' \quad products \tag{1-54}$$

By considering the mass balance for hydrogen in the differential volume element **figure (1-11),** from the gas bubbles to reaction surface and its consumption by catalyst, **Deckwer et al. [1981]** obtained the following relation:

$$-\frac{d(U_G\, y)}{dZ_L} = \frac{RT\, y}{m'_{H_2}} \left[\frac{1}{a\, k_{L,H_2}} + \frac{1}{k'_c\ \varepsilon_L} \right] = \frac{k_0\ RT\, y}{m'_{H_2}} \tag{1-55}$$

where Z_L axial distance, m

Further

$$U_G = U_{G0} \quad \left\{ 1 \ + \ X_{H_2} \left[\alpha\ (1+U)\ \frac{C_{H_2,G0}}{C_{CO,G0} + C_{H_2,G0}} \right] \right\} \tag{1-56}$$

And

$$y = y_{G0}\ \ (1 - X_{H_2})(U_{G0}/U_G) \tag{1-57}$$

Equation (1-55) with equations. (1-56) and (1-57) finally yield:

$$\alpha^*\, X^e_{H_2} + (1+\alpha^*)\ln(1 - X^e_{H_2}) = k_0\, L/(U_{t,G0}\ m''_{H_2}) \quad = \quad St \tag{1-58}$$

In this treatment the variation of gas velocity with the overall conversion was considered and this volume contraction was defined in terms of a contraction factor α_C, such that

$$\alpha_C \quad = \quad [Q\,(X_{H_{2+CO}} = 1) \ - \ \dot{Q}^m\ ]\ /\ \dot{Q}^m \tag{1-59}$$

The modified gas contraction factor α^* is related to α_c by the following relation:

$$\alpha^* = \alpha_C(1+U) / (1+I) \qquad (1\text{-}60)$$

where

$I = C_{CO,G0} / C_{H_2,G0}$

On the basis of this formulation, **Deckwer et al. [1981] model** claimed that the Fischer-Tropsch slurry process in bubble columns is mainly controlled by reaction resistance. Mass transfer limitations are negligible for the known catalysts and appropriate operating conditions. This is a consequence of the high hold up for the gaseous phase in the liquid phase of molten paraffin.

1-3-3-Mathematical Model of Deckwer [1982]

Deckwer et al. [1982] have developed a sophisticated model in which the flow patterns in both the gas phase and the liquid phase are accounted for in terms of axial dispersion. This model is also the first one to consider the heat transfer effect and the sedimentation of solid catalyst in the slurry phase. They also consider the liquid-solid mass transfer resistance and the catalyst loading in the kinetic rate expression. These workers do not consider the various product species and confine themselves to the task of evaluating hydrogen conversion only.

Model assumptions:

1- There is axial dispersion in the gas and the liquid phases.
2- The catalyst is not uniformly distributed over the entire suspension volume, which is considered by introducing the sedimentation dispersion model.
3- The rate-limiting step is first order in H_2 and zero order in CO as proposed by **[Dry, 1976 and Atwood and Bennett, 1979]** and successfully applied by **[Satterfield and Huff, 1980 and Deckwer et al., 1981].**

4-Absorption enhancement at the gas-liquid interface due to chemical reaction on the surface of fine catalyst particles can be neglected

5-The unknown stoichiometry of the FT synthesis will be considered by introducing the usage ratio U.

6-The total pressure within the reactor is constant; i.e., the influence of hydrostatic head on gas expansion is neglected.

7-The variability of the molar gas flow rate will be accounted for by applying a contraction factor α_C . It varies between –0.5 and –0.6

8-The hydrodynamic properties, i.e., gas hold up, interfacial area, heat and mass transfer coefficients, and dispersion coefficients, are assumed to be spatially independent.

9- Owing to the low heat capacity of the gas phase compared to the slurry phase a heat balance on the suspension (liquid plus solid) will only be considered.

10-Preliminary calculations have indicated that the temperature profiles within the slurry phase is flat. Therefore, the variation of the physicochemical properties (i.e., density, viscosity, diffusivity, and solubility) with temperature along the reactor is not considered. The physicochemical properties are calculated for the mean reactor temperature. The temperature influence on the gas flow rate within the reactor is also neglected.

11-As the catalyst particles are usually small, pore diffusion limitations are neglected. In addition, no temperature difference between the catalyst and the liquid is assumed.

Model equations

As the rate of synthesis gas conversion depends only on the hydrogen concentration in the liquid phase, the balance equations need only to be formulated for this key component.

At steady state, by considering the net flow of hydrogen into a differential volume element by axial dispersion and convective flow and equating it to the rate of mass transfer from the gas-liquid interface to the

bulk liquid in relation to **figure (1-11), these workers [1982]** derived the following relations.

The gas phase mass balance is therefore:

$$\left(\frac{1}{Bo_G}\right)\left(\frac{d^2\bar{y}}{d\,Z^2}\right) - [(1+\alpha^*)\ /\ (1+\alpha^*\,\bar{y})^2]\ (d\,\bar{y}/dZ) - St_G\ \theta\ (\bar{y}-\bar{x}) = 0 \qquad (1\text{-}61)$$

where

Z = reduced axial distance, dimensionless

$$\bar{y} = y / y_{G0}$$

$$\theta = T/T_C$$

$$St_G = a\,k_{L,H_2}\,R\,L\,T_C / m'_{H_2}\,U_{G0}$$

$$\bar{x} = C_{H_2,L} / C^*_{H_2,L} = C_{H_2,L}\,m''_{H_2} / C_G\,y_{G0}$$

And

$$Bo_G = U_{G0}\,L / D_G\,\varepsilon_G$$

The liquid phase mass balance can be written as:

At the steady state, the liquid mass balance **figure (1-11)** yielded the following relation:

$$(\frac{1}{Bo_L})\ (\frac{d^2\bar{x}}{d\,Z^2}) + St_L\ (\bar{y}-\bar{x}) - Da'\,\eta_s(\theta)\ W(Z)\exp(-\delta/\theta)\,\bar{x} = 0 \qquad (1\text{-}62)$$

Here

$$Bo_L = U_{G0}\,L / D_L\,\varepsilon_L$$

$$St_L = a\,k_{L,H_2}\ L/U_{G0}$$

$$\eta_S(\theta) = [1+\eta_{S0}\ \exp(\frac{-\delta}{\theta})]^{-1}$$

$$\eta_{s0} = k_f\ \overline{W}\ \varepsilon_L / (k_s\ \bar{a}_s)$$

$$Da' = k_f\ \varepsilon_L\ L/U_{G0}$$

$$\delta = E_A / RT_C$$

The steady state the heat balance in the slurry reaction was formulated on the basis that the net heat flux into the differential volume element by thermal conduction, and the heat generated within the element due to chemical reaction will be equal to the rate of heat removal at the cooling surface.

The energy balance can be written as:

$$\left(\frac{1}{Pe}\right)\left(\frac{d^2\theta}{d\,Z^2}\right) - St_H\,(\theta - 1) + Be\;Da'\;[1 + \eta_{SO}\exp(-\delta/\theta)]^{-1}\,W(Z)\exp(-\delta/\theta)\,\bar{x} = 0 \qquad (1\text{-}63)$$

Here

$$Pe = U_{G0}\,\rho_{SL}\,Cp_{,SL}\,L/\lambda_{SL}\,\varepsilon_L \qquad : \quad St_H = h\,a_h\,L\,/\,U_{G0}\,\rho_{SL}\,C_{P,SL}$$

$$Be = (-\Delta H_R)P\;y_{G0}\;/\rho_{SL}\,C_{P,SL}\,m'_{H_2}\,T_C \qquad \text{and} \qquad \bar{x} = C_{H_2,L}\;m'_{H_2}\,/\,P\;\;y_{G0}$$

The knowledge of catalyst concentration distribution in the slurry reactor, $W(\zeta)$, is essential as it occurs both in equations (1-62) and (1-63), and **Deckwer et al. [1982]** determined it on the basis of a sedimentation-dispersion model. A mass balance for catalyst particles over the volume element of **figure (1-11)** can be formulated on the basis that the net flux of catalyst particles into a differential volume element by axial dispersion and hindered settling will be equal to the rate of particle accumulation within the element. **At steady state, the final result is:**

$$W(Z) = \overline{W}\;Bo_C\;\exp(-Bo_C\;Z)\,[\,1 - \exp(-Bo_C)\,]^{-1} \qquad (1\text{-}64)$$

Here $\qquad Bo_C = U_t\,L\,/\,D_C$

The four equations, (1-61), (1-62), (1-63) and (1-64) representing the hydrogen balance in the gas and liquid phases, heat balance in the reactor, and the catalyst concentration profiles, respectively, describe the mathematical model of **Dckwer et**

al. [1982]. The three differential equations, (1-61), (1-62) and (1-63) could be solved in conjunction with the boundary conditions discussed below:

For the flowing gas stream, mass transfer from the bubbles to the slurry will cease at the reactor outlet, resulting in the boundary condition that:

$$at \quad Z=1 \quad ; \quad \frac{d\bar{y}}{dZ}=0$$

Lastly, by continuity, the rate at which hydrogen enters the reactor in the feed gas plus the rate at which hydrogen is transported to the reactor inlet by axial dispersion must equal the rate at which hydrogen is transported away from the reactor inlet by convective flow. Therefore:

$$at \quad Z=0: \qquad A\,U_{G0}\;C_{H_2,G0} \;+\; A\,D_G\,\varepsilon_G\,(dC_{H_2,G}/dZ) \;=A\,U_G\,C_{H_2,G} \qquad (1\text{-}65)$$

This after several substitutions from the foregoing relations can be manipulated to the following:

$$at \quad Z=0: \qquad \left((1+\alpha^*)\bar{y}/(1+\alpha^*\bar{y})\right) \;-\; (1/Bo_G)\,(d\bar{y}/dZ) \;=\; 1 \qquad (1\text{-}66)$$

1-3-4-Mathematical Model of Satterfield (1980)

Satterfield and Huff [1980] based their mathematical development on the assumption that the slurry phase is completely backmixed. The other assumptions implicit in their work are the same as mentioned in the beginning of the **[Calderbank et al. 1963]** model. Satterfield and Huff have neglected the effect of conversion on superficial gas velocity and considered the volumetric gas flow rate to be constant along the reactor height. The effect of catalyst loading is accounted for while modeling the reaction kinetics. The hydrogen balance gave finally:

$$C^e_{H_2,G} = C_{H_2,G0}\exp(-\alpha_{H_2}\;L) + m''_{H_2}\,C_{H_2,L}[1-\exp(-\alpha_{H_2}\,L)] \qquad (1\text{-}67)$$

Here

$$C_{H_2,G} = m''_{H_2}\,C^*_{H_2,L}$$

$$m''_{H_2} = m'_{H_2}/RT \;=\; m_{H_2}/RT\;C_L$$

and

$$\alpha_{H_2} = a\ k_{L,H_2} / m''_{H_2}\ U_G$$

With reference to **figure (1-11)** the overall rate of hydrogen absorption per unit volume of expanded slurry phase was expressed as:

$$R_{H_2} = (Q/V)(C_{H_2,G0} - m''_{H_2}\ C_{H_2,L})[1 - \exp(-\alpha_{H_2}\ L)] \tag{1-68}$$

$C_{H_2,L}$ was determined by performing an overall mass balance for carbon monoxide and hydrogen around the reactor. By equating the overall rate of absorption of CO and H_2 per unit volume of expanded slurry to the reactions that occur at the catalyst surface, they obtained:

$$R_{H_2+CO} = k''_c\ (1-\varepsilon_G)\ W\ C_{H_2,L} \tag{1-69}$$

Where k''_c is the kinetic rate constant for CO and H_2 consumption referred to the catalyst loading in the slurry. $C_{H_2,L}$ was given by

$$C_{H_2,L} = \left[\frac{R_{H_2}(C_{R,G0} - C^e_{R,G})}{(C_{H,G0} - C^e_{R,G})\ k''_c\ (1-\varepsilon_G)\omega}\right] \tag{1-70}$$

Substituting for $C_{H_2,L}$ from equation (1-70) in equation (1-68) gave the desired relation after some manipulation as:

$$\frac{VX^e_{H_2}}{m''_{H_2}\ Q(1+I)\ X^e_{H_2+CO}\ [1-\exp(-\alpha_{H_2}L)]} + \frac{1}{k''_c\ (1-\varepsilon_G)\omega} = \frac{V}{m''_{H_2}\ Q(1+I)\ X^e_{H_2+CO}} \tag{1-71}$$

Here

$$X_{H_2} = (C_{H_2,G0} - C^e_{H_2,G})/C_{H_2,G0}$$

$$X_{H_2+CO} = (C_{R,G0} - C^e_{R,G})/C_{R,G0}$$

$$C_{R,G0} = C_{H_2,G0} + C_{CO,G0}$$

Satterfield and Huff [1980] interpreted the right side of equation (1-71) as the total resistance, and the two terms on the left side of equation (1-71) as the mass transfer and kinetic resistances, respectively.

1-3-5-Mathematical model of Bukur [1983]

Bukur [1983] proposed a model along the same lines as that of **[Satterfield and Huff , 1980]** except he considered the effect of gas contraction on superficial velocity in a fashion similar to that of **[Deckwer et al., 1981].** He considered the same kinetic and mass transfer resistances as in the above models but did not include the catalyst loading factor in his kinetic rate expression as done by **[SatterfielSd and Huff, 1980].** His final expression for the gas-phase mass balance was:

$$\frac{L\ ak_{L,H_2}}{U_{G0}\ m''_{H_2}} = \frac{-1}{(1+\alpha^*\ X_G)}\ [\alpha^* X^e_{H_2} + (1+\alpha^* Y)\ \ln\{1-(X^e_{H_2}/Y)\}] \qquad (1\text{-}72)$$

Here

$$Y = (1-X_G)/(1+\alpha^*\ X_G)$$

And

$$X_G = C_{H_2,L}\ \ m''_{H_2}/C_{H_2,G0} = \theta_{H_2,L}$$

$\theta_{i,L}$ notation is more convenient in considering the multicomponent transport process and was used by **[Stern et al., 1983]. Bukur [1983]** introduced an overall hydrogen balance to eliminate $C_{H_2,L}$ in equation (1-72) and expressed it in the following final form:

$$\frac{L\ ak_{L,H_2}}{U_{G0}\ m''_{H_2}} = \frac{-1}{1+(\alpha^* X^e_{H_2}/N_R)}$$

$$\left[\ \alpha^* X^e_{H_2} + \left\{1+\alpha^*\ \frac{1-(X^e_{H_2}/N_R)}{1+(\alpha^* X^e_{H_2}/N_R)}\right\}\ \ln\left\langle 1-X^e_{H_2}\ \frac{1+(\alpha^* X^e_{H_2}/N_R)}{1-(X^e_{H_2}/N_R)}\right\rangle\ \right] \qquad (1\text{-}73)$$

Where

$$N_R = L\ k'_C\ \varepsilon_L/m''_{H_2}\ U_{G0}$$

N_R number of reaction units, dimensionless

1-3-6-Mathematical Model of Stern [1983]

The Stern et al. [1983], mathematical formulation is based on the same assumptions mentioned in the beginning. **They** developed a model in which the liquid phase was assumed to be completely backmixed and the catalyst particles to be uniformly dispersed in the liquid phase. Gas contraction was considered according to a procedure different from that of **[Deckwer et al., 1981].** Further, in this model the mass transfer of both hydrogen and carbon monoxide were considered. Another special feature of this work was in the inclusion of the resistance offered to the transport of products from the bulk liquid to gas phase through the gas-liquid interface. Methane synthesis was taken to model the reaction stoichiometry. The catalyst loading was included in the kinetic rate expression, and the rate of removal of a component from the reactor with the liquid product stream was accounted for in the liquid-phase mass balance. As in other models, the gas-liquid mass transfer and chemical reaction were considered as the rate-controlling steps.

The mass balance for a component i, an overall gas-phase mass balance, an average gas-phase concentration for a component i, and a liquid-phase mass balance were considered to obtain the following final four relations describing the model:

The gas phase mass balance for each component:

$$-d(\bar{v}\,\theta_{i,G})/dZ = St_{i,G}\,(\theta_{i,G}-\theta_{i,L}) \qquad (1\text{-}74)$$

Further,

$$\theta_{i,G} = C_{i,G}/C_{H_2,G0}$$

$$\theta_{i,L} = C_{i,L}\; m_i''\; /C_{H_2,G0}$$

$$\theta_G = C_G/C_{H_2,G0}$$

$$St_{i,G} = a\,k_{L,i}\,L/m_i''\;U_{G0}$$

$$m_i'' = m_i'\;/RT \;=\; m_i/RT\;C_L$$

$$-\theta_G \; d\bar{v}/dZ \; = \sum_{i=1} St_{i,G} \; (\theta_{i,G} - \theta_{i,L}) \qquad (1\text{-}75)$$

The average gas phase concentration for each component i is defined as:

$$\bar{\theta}_{i,G} = \int_0^1 \theta_{i,G} \; dZ \qquad (1\text{-}76)$$

The liquid phase mass balance for each component (the liquid is completely mixed) is given by:

$$-\theta_{i,L} + St_{i,G} \; m_i'' \; (\tau_L / \tau_G)(\bar{\theta}_{i,G} / \bar{\theta}_{i,L}) = \gamma_i \; Da \; (\tau_L \; m_i'' \; / \tau_G \; m_{H_2}'') \; \theta_{H_2,L} \qquad (1\text{-}77)$$

The boundary conditions at $Z = 0$ are:

$U_G = U_{G0}$ and $C_{i,G} = C_{i,G0}$

Here

Damkohler number, Da, was defined as:

$Da = L \; W(1-\varepsilon_G) k_c / U_{G0}$

γ_i is the stoichiometric coefficient for component i

$\bar{v} = U_G / U_{G0}$

Equations (1-75), (1-76) and (1-77), together with the boundary conditions, could be solved numerically to establish the variation of gas and slurry phase concentration along the reactor height for different values of the controlling parameters.

1-3-7-Mathematical Model of Stern [1985]

Model assumptions and features

1-There is axial dispersion in the gas and liquid phases.

2-The catalyst is not uniformly distributed over the entire suspension volume.

3-The influence of H_2 and CO concentrations in the liquid phase on the stoichiometry and kinetics of the synthesis and water gas shift reactions are treated rigorously.

4- The model is used to establish the influence of transport parameters on syngas conversion and the axial distributions of reactant and product concentrations in both the gas and liquid phases, for a reactor operated with an iron catalyst.

5-The model is used to describe the performance of the bubble column reactors described by **[Deckwer et al., 1982]**

The gas phase mass balance:

$$\frac{\varepsilon_G}{Pe_G}\frac{d^2\theta_{i,G}}{dZ^2} - \frac{d(\bar{v}\theta_{i,G})}{dZ} - St_{i,G}(\theta_{i,G} - \theta_{i,L}) = 0 \qquad (1\text{-}78)$$

The boundary conditions on equation (1-78) are:

$$\theta_{i,G} - \frac{\varepsilon_G}{Pe_G}\frac{d\theta_{i,G}}{dZ} = \theta_{i,G0} \qquad at \qquad Z = 0$$

$$\frac{d\theta_{i,G}}{dZ} = 0 \qquad at \quad Z = 1$$

The dependence of $\bar{v}$ on Z is determined by using the following overall mass balance

$$\theta_G \frac{d\bar{v}}{dZ} + \sum_{i=1}^{n} St_{i,G}(\theta_{i,G} - \theta_{i,L}) = 0 \qquad (1\text{-}79)$$

The boundary condition on equation (1-79) is:

$$\bar{v} = 1 \qquad at \quad Z = 0$$

where $$Pe_G = \frac{U_{G0}\,L}{D_G}$$

The liquid phase mass balance for each component is given by:

$$\frac{\varepsilon_L}{Pe_L}\frac{d^2\theta_{i,L}}{dZ^2} - \frac{d\theta_{i,L}}{dZ} + St_{i,L}(\theta_{i,G} - \theta_{i,L}) + \frac{m_i''\,W(1-\varepsilon_G)\,L}{C_{H_2,G0}\,U_{G0}}R_i = 0 \qquad (1\text{-}80)$$

or

$$\frac{\varepsilon_L}{Pe_L}\frac{d^2\theta_{i,L}}{dZ^2} - \frac{d\theta_{i,L}}{dZ} + St_{i,L}(\theta_{i,G} - \theta_{i,L}) + m_i'' \omega(v_i Da_L \theta_{H_2,L} + v_i' Da_L' (\theta_{H_2O,L}\theta_{CO,L} - \frac{1}{K'}\theta_{CO_2,L}\theta_{H_2,L})] = 0 \quad (1\text{-}81)$$

The appropriate boundary conditions for equations (1-80 and 1-81) are

$$\theta_{i,L} - \frac{\varepsilon_L}{Pe_L}\frac{d\theta_{i,L}}{dZ} = \theta_{i,L0} \qquad at \quad Z = 0$$

$$\frac{d\theta_{i,L}}{dZ} = 0 \qquad at\ Z = 1$$

$$D_{aG} = \frac{k_{FTS}\omega(1-\varepsilon_G)L}{U_{G0}m'_{H_2}} \qquad D_{aL} = D_{aG}\frac{U_{G0}}{U_L}$$

Here

$$D'_{aG} = \frac{k_{WGS}\omega(1-\varepsilon_G)C_{G0,H_2}L}{U_{G0}m'_{H_2O}m_{CO}} \qquad D'_{aL} = D'_{aG}\frac{U_{G0}}{U_L}$$

$$St_{i,L} = \frac{a k_{L,i} L}{U_L} \qquad Pe_L = \frac{U_L L}{D_L} \qquad \text{and} \qquad \omega = \frac{W}{\overline{W}}$$

The axial distribution of catalyst is governed by gravitational settling and axial dispersion due to agitation of the catalyst slurry by the gas flow. Assuming that the volume fraction of liquid is essentially constant along the column length.

The mass balance catalyst can be written:

$$Pe_C^{-1}\frac{d^2\omega}{dZ^2} + \frac{d\omega}{dZ} = 0 \quad (1\text{-}82)$$

The boundary condition on equation (1-82) is

$$W - Pe_C^{-1}\frac{dW}{dZ} = 0 \qquad at\ Z{=}0 \qquad \int_0^1 \omega\, dZ = 1$$

Here $Pe_C = \frac{L}{D_S}\left[\frac{U_{ST} - U_L}{\varepsilon_L}\right]$

1-3-8-Mathematical Model of Shah et al., (1985)

Model assumptions:

1- The bubble column reactor operating in the churn- turbulent flow regime

2- The gas flow can be broken down approximately in terms of transport flow (i.e., flow by large bubbles) and entrained flow (i.e., flow by small bubbles) **Vermeer and Krishna, [1981]**

3- The large bubbles rise much faster through a swarm of small bubbles and can be assumed to rise in a plug flow manner **Vermeer and Krishna, [1981]**

4- The small bubbles are assumed to be completely back mixed.

5- No interaction between the two bubbles classes is considered.

6- Assume a gas –liquid reaction.

7- The catalyst is assumed to be uniformly distributed in the liquid phase.

8- The rate of reaction is only dependent on the liquid phase concentration of component, i and is assumed to be first order for H_2.

9- The pressure in the reactor is assumed to be constant.

10- The liquid- solid mass transfer resistance is assumed to be negligible

11- The kinetic constant includes the catalyst concentration in the slurry phase.

12- The equilibrium liquid phase concentration of component, i for small and large bubbles will be assumed to follow Henry's law.

13- The concentration of component, i in the large bubbles varies along the length of the column

The gas phase mass balance for component *i* in the *large* bubbles, rising in plug flow is:

$$-\frac{d\left(U_{LB}\, y_{i,G}^{large}\, P\,/RT\right)}{dZ} = (k_i a)_i^{large}\left(C_{i,L}^{*large} - C_{i,L}\right) \qquad (1\text{-}83)$$

With concentrations in mol/m^3 subject to the boundary conditions at the reactor entrance: Z=0: $C_{i,G}^{large} = C_{i,G0}$.

The gas phase mass balance for component *i* in the *small* bubbles (completely mixed) is:

$$U_{DF}(y_{i,G0} - y_{i,G}^{small}) = L\ (k_L a)_i^{small} \frac{RT}{P}(C_{i,L}^{*small} - C_{i,L}) \qquad (1\text{-}84)$$

The mass balance for component *i* in the completely mixed liquid phase can be written as:

$$(k_L a)_i^{large} \int_0^1 \left(C_{i,G}^{*large} - C_{i,L}\right) dZ + (k_L a)_i^{small} \left(C_{i,L}^{small} - C_{i,L}\right) - k_A\, \varepsilon_l\, C_{i,L} = 0 \qquad (1\text{-}85)$$

Where

$$C_{i,L}^{*small} = \frac{P\ y_{i,G}^{small}}{m_i'} \qquad C_{i,L}^{*large} = \frac{P\ y_G^{large}}{m_i'}$$

$$U_{LB} = U_{br}^{large}\ \varepsilon_G \qquad U_{DF} = U_{br}^{small}\ \varepsilon_G$$

1-3-9-Mathematical Model of Van der Laan et al. (1999)

This model is based on the same assumptions as that of **Shah et al. [1985]** the balances for gas and liquid phases are essentially the same see **figure (1-12),** more over the model takes into consideration heat effects, both the Fischer-Tropsch reaction and the water gas shift reaction and the olefins and paraffins distribution in the products. This model will be subjected to more elaboration in the next chapter.

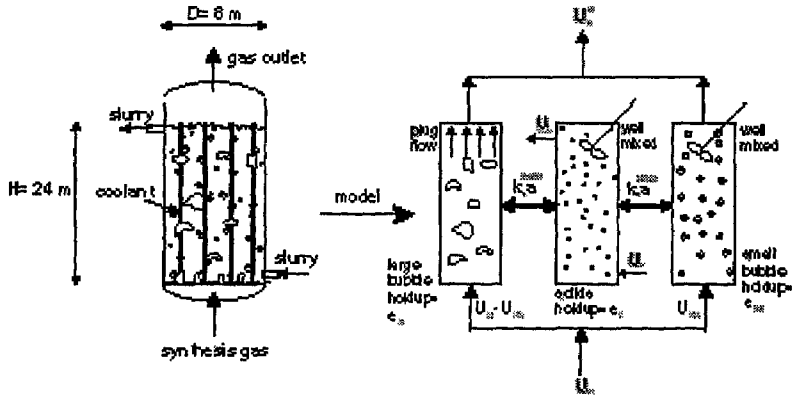

Figure (1-12) Hydrodynamic model of slurry bubble column reactor in the heterogeneous flow regime.